This is to certify that the

thesis entitled

Stress Relaxation In Lead-Free Solder Joints

presented by

Susheel Ganeshrao Jadhav

has been accepted towards fulfillment
of the requirements for

Masters degree in Materials Science and Engineering

S. N. Subramanian

Major professor

Date 4/11/2001

STRESS RELAXATION IN LEAD-FREE SOLDER JOINTS

BY

SUSHEEL GANESHRAO JADHAV

A THESIS

Submitted to
Michigan State University
in partial fulfillment of the requirements
for the degree of

MASTER OF SCIENCE

Department of Materials Science and Mechanics

2001

ABSTRACT

STRESS RELAXATION IN LEAD-FREE SOLDER JOINTS

BY

SUSHEEL GANESHRAO JADHAV

Stress relaxation experiments were carried out at 25°C and 150°C on 96.5Sn-3.5Ag eutectic solder and Sn-Ag composite solder (Sn-Ag eutectic solder with 20%volume Cu_6Sn_5 reinforcements incorporated by *in-situ* methods.) The magnitude of stress drop during relaxation depends upon the plastic shear strain imposed prior to the stress relaxation process. For sequential stress relaxation experiments that include unloading, stress drop is nearly independent of the accumulated plastic shear strain. However, for sequential stress relaxation that does not involve unloading, the stress relaxation is dependent upon the cumulative plastic shear strain. Stress relaxation behavior in shear is different than stress relaxation in tension. Creep rates extracted from the relaxation data were much faster with larger pre-strains in both eutectic Sn-Ag and composite solder joint. The stress exponent values (n) calculated from the stress relaxation test data ranged from 7 to 15 for both eutectic as well as composite solder joints suggesting that the deformation mechanism active during the observed stress relaxation may be controlled by dislocation climb recovery processes.

To Aai and Pappa

ACKNOWLWDGEMENTS

I thank my advisor Prof. K.N. Subramanian for his substantial help and guidance throughout the project. I gratefully acknowledge Profs. T.R. Bieler and J. P. Lucas for their constant encouragement and support in this project.

Also my sincerest thanks to Dr. D. Y. Seo, F. Guo, T. Lagrange and S. Choi for their help in making me familiar with the equipment that I needed for this project. My thanks to department technician K. Niemeyer for his help on the preparation of the equipment.

Finally, I thank Composite Materials and Structures Center of the Michigan State University for the financial support of this project.

TABLE OF CONTENTS

LIST OF TABLES

LIST OF FIGURES

PAGE

INTRODUCTION

Soldering may be defined as the joining of materials using a filler material which forms a bond (usually intermetallic) with the substrates being joined. The soldering process is generally regarded as being restricted to temperatures below 450^{0}C. Although this process has been used since Roman times, the use of solder joints in microelectronic circuits has led to a sustained interest in the detailed study of the behavior of solders. With the rapid growth of information technology, the mircoelectronics sector is becoming one of the largest industrial sectors and solder joint technology is expected to play an important role in the development of electronic systems. In addition, growing consumer demand for faster computers had led to the miniaturization of printed circuit boards (PCBs). This has led to a greater emphasis on the solder joint reliability as the solder joint has to perform the role of a mechanical as well as electrical connection between the printed circuit board and the device especially in currently popular surface mount configuration.

Table 1 shows the commonly used Pb containing solder alloys. Due to the environmental hazards posed by the presence of toxic lead in the solder, the microelectronics industry is moving towards the use of lead-free solders. In the meantime, the continued trend towards the miniaturization of printed circuit boards and interconnect miniaturization in surface mount technology (SMT) is stretching the physical capability of solder to provide sound and reliable joints [1].

Table 1. Melting points of various lead-free alloys. Adapted from [1].

Alloy Composition (wt %)	T_m °C	T_s °C	T_l °C	T_e °C
Bi-26In-17Sn	79			
Bi-32Sn				109.5
Bi-41.7Sn-1.3Zn	127			
Bi-43Sn(eutectic)				139
Bi-45Sn-0.33Ag	140-145			
In-3Ag				141
In-34Bi				110
In-48Sn(eutectic)				117
Sn-1Ag-1Sb		222	232	
Sn-2.5Ag-0.8Cu-0.5Sb	210-216		217	
Sn-2.8Ag-20In	178			
Sn-25Ag-10Sb	233			
Sn-2Ag-0.8Cu-0.6Sb	210-216			
Sn-2Ag-0.8Cu-6Zn		217	217	
Sn-3.5Ag(eutectic)				221
Sn-3.5Ag-1Zn	217			
Sn-3.6Ag-1.5Cu	225			
Sn-4Ag		221	225	
Sn-4Ag-7Sb			230	
Sn-10Bi-0.8Cu		185	217	
Sn-10Bi-5Sb		193	232	
Sn-42Bi		139	170	
Sn-45Bi-3Sb		145	178	
Sn-57Bi-1.3Zn	127			
Sn-0.7Cu(eutectic)				227
Sn-2Cu-0.8Sb-0.2Ag	266-268			
Sn-3Cu		227	275	
Sn-4Cu-0.5Ag		216	222	
Sn-20In-2.8Ag	178-189			
Sn-42In		117	140	
Sn-36In		117	165	
Sn-50In		117	125	
Sn-8.8In-7.6Zn	181-187			

Thus clean environmental requirements coupled with the need for solders with better creep and fatigue resistance are forcing PCB manufacturers worldwide to look for Pb-free solder alternatives [2].

A relatively large number of lead free solder alloys have been proposed and they are listed in **Table 2** [1]. The performance requirements of these lead free alloys used in the microelectronics are severe. From the manufacturing point of view properties such as melting/liquidus temperature, wettability with Cu, cost, availability, manufacturability using current processes and ability to be made into balls/paste are some of the important issues. Properties such as electrical conductivity, thermal conductivity, intermetallic compound formation, coefficient of thermal expansion, shear properties, creep properties and thermomechanical fatigue are important for the reliability and performance issues [1].

Reliability issues in electronic solder joint technology

Since the solder joints act as an electrical as well as the mechanical connection in a soldered assembly, their mechanical characteristics are important considerations for their functionality. The mechanical properties may be categorized into three broad categories: time-independent monotonic deformation, time-dependent monotonic deformation (creep) and cyclic deformation (fatigue).

Temperature fluctuations, and to a lesser extent, mechanical vibrations during service, are the principal factors affecting the reliability of the solder joint.

Table 2. Composition of various lead-free alloys. Adapted from [1].

Alloy Composition (wt. %)	Liquidus (^{0}C)	Solidus (^{0}C)	Tensile Strength (MPa)	0.2% Proof Strength(MPa)	Elongation (%)
63Sn-37Pb	183	183	35.4	16.1	1.4
60Sn-40Pb	190	183	28	14.2	5.3
25Sn-75Pb	266	183	23.1	14.2	8.4
10Sn-90Pb	302	268	24.3	13.9	18.3
5Sn-95Pb	312	308	23.2	13.3	26
80Sn-20Pb	199	183	43.2	29.6	0.8
95Pb-5In	314	292	25.2	13.9	33
70Pb-30In	253	240	33.3	24.7	15.1
95Pb-5Sb	295	252	25.6	16.9	13.7
85Pb-10Sb-5Sn	255	245	38.4	25.3	3.5
88Pb-10Sn-2Ag	290	268	27.2	15.5	15.9
97.5Pb-1Sn-1.5Sg	309	309	38.5	29.9	1.15
85Sn-10Pb-5Sb	230	188	44.5	25	1.4

A pronounced difference in the coefficient of thermal expansion (CTE) between substrate material and the device as a consequence of heat generated within the device during operation of the instrument and the temperature changes which stem from the external operating environment cause cyclic thermal strains in the solder joint (**Table 3**)[3]. For example, a commonly used substrate epoxy glass FR-4 board has a CTE of $15x10^{-6}$/ K whereas the CTE of a solder such as Sn-Ag is $23x10^{-6}$/ K and the CTE of Si is about $3x10^{-6}$/ K (**Table 4)**[1]. When the device undergoes thermal cycling various materials in the device undergo thermal expansion or contraction to different extents, generating thermal strains. Just as the CTE mismatch between various components of an electronic package causes thermal fatigue, thermally induced deformation within solder alloys themselves has also been observed, and is ascribed to CTE mismatches between crystallographic grains and phases within the solder alloy [4]. It is important to be aware of such deformation during the evaluation of lead-free alternatives for use in the electronic packages to ensure that the internal CTE mismatch in these solders is minimized.

Also, the inherent low melting point of the solder desirable for the process compatibility with the polymeric materials used in the PCB has led to a disadvantage because the room temperature itself represents a high homologous temperature for the solders used. **Figure 1** [3] shows the severity of typical service conditions for solders (homologous temperature up to 0.9 T_m) as compared to other 'high' temperature alloys. Thus time dependent effects such

Table 3. Temperature limits and performance requirements for electronic assemblies. Adapted from [3].

Application	$T_{min.}$	$T_{max.}$	ΔT	Dwell	Cycles	Lifetime
	(^{0}C)	(^{0}C)	(^{0}C)	(hours)	(per year)	(years)
Consumer	0	60	60	12	365	1-3
Computers	15	60	45	2	1460	4-5
Telecommunications	-40	85	125	12	365	7-20
Commercial Aircraft	-55	95	150	2	3000	8-10
Motor Vehicle (passenger compartment)	-55	65	120	12	100	8-10
Motor vehicle (engine compartment)	-55	125	180	1	300	4-5
Space (low earth orbit)	-40	85	125	1	8760	5-20
Military avionics	-55	95	150	2	500	4-5

Table 4. Coefficient of Thermal Expansion values of different materials used in the printed circuit boards. Adapted from [1].

Composition	CTE (10^{-6}/K)
Bi-42Sn	15 at 20°C
In-48Sn(eutectic)	20 at 20°C
Sn-3.5Ag	23
Sn-4.8Bi-3.4Ag	23
Sn-20In-2.8Ag	28 at 20°C
Sn-37Pb	21
In-3Ag	20
Si	2.6
Cu	16-18
Epoxies	60-80
FR-4	11-15

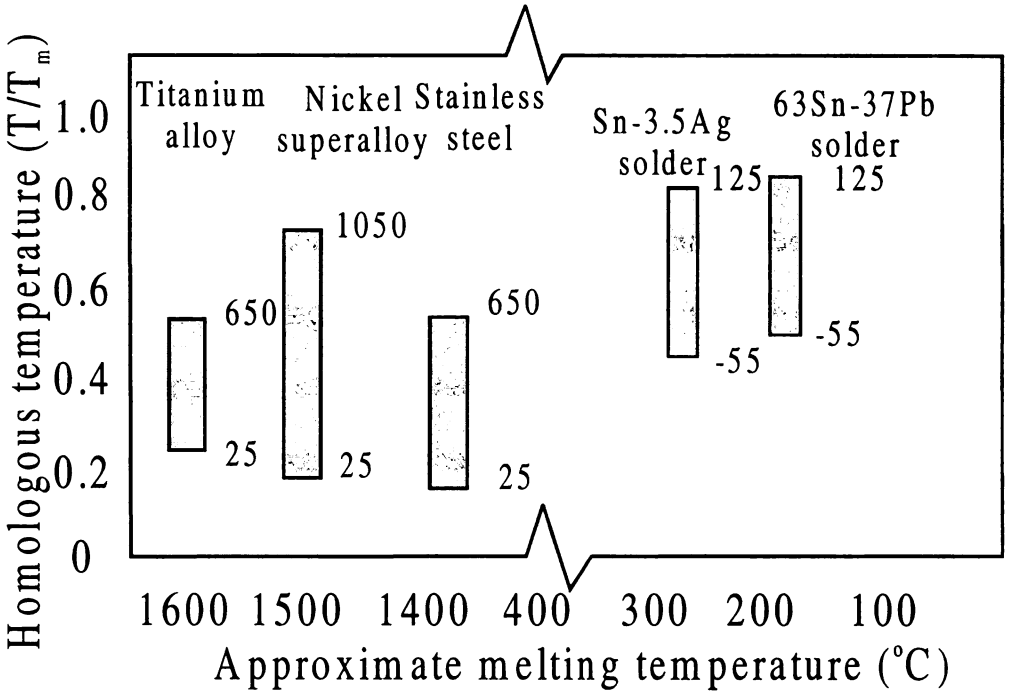

Figure 1. Comparison of homologous temperature of various alloys under service conditions. Adapted from [3].

as creep, stress relaxation and thermomechanical fatigue (TMF) are important parameters for the reliability prediction of the solder joints.

Aim of the Study

The aim of this study is to characterize the stress relaxation behavior of Sn-Ag solders. During TMF, damage is sustained by the solder joint during the relaxation process occurring at dwell periods. The effect of damage sustained by the solder joint during relaxation process needs to be quantified in order to accurately model the TMF behavior of the solder joints. The effect of tensile dwell period versus compressive dwell period on the solder joint relaxation process is also an important parameter to be characterized. The question that needs further probing is whether stress relaxation is a stress dominated or a strain dominated event. In this study, an attempt was made to find solution to some of these questions.

LITERATURE REVIEW

Creep of solder joints

Creep is a measure of time required for a material to fail when it is under a constant load at high homologous temperature (T_h>0.5T_m). It involves deformation mechanisms such a grain boundary sliding, vacancy diffusion etc. for which thermal energy is the main driving force. Hence, creep deformation becomes critical when the operating temperature exceeds half the absolute melting temperature of the material. When a material is subjected to constant load at high temperature it exhibits three regions of creep behavior known as primary, secondary and tertiary creep. The creep rate in the secondary stage called as steady-state creep rate is the most relevant because it has the simplest and the most reproducible behavior from which deformation mechanisms have been uncovered [5]. The simplest form of creep equation in the secondary steady-state creep region is given by [6]

$$\frac{d\gamma}{dt} = A\tau^n \exp\left(-\frac{\Delta H}{RT}\right).$$

where, $\frac{d\gamma}{dt}$ is shear strain rate, τ is shear stress, n is the stress exponent and ΔH is the activation energy for creep, A is a constant, R is universal gas constant and T is the absolute temperature (K). The activation energy and stress exponent for the secondary creep rate are associated with the rate controlling process for the secondary creep, and can provide an insight into the operative creep mechanism of the material. In eutectic Pb-Sn solder, the rate controlling mechanism at strain rates below 10^{-5} s^{-1} is lattice self-diffusion which also

appears to be the case with Sn-Bi solder [6]. Mei and Morris [5] observed that at 65^{0}C solder joints made with eutectic Sn-Bi are more creep resistant than eutectic Pb-Sn under the same conditions. Tests conducted by Frear and Morris [7] to evaluate the creep behavior of eutectic In-Sn solder indicated rapid and extensive deformation leading to early failure. In their studies, In-Sn solder did not show microstructural changes such as coarsening and recrystallisation during creep as observed with Pb-Sn solder. Darveaux and Bannerji's [8] test results also suggested that the acceleration factor in a thermal cycling test may be greater for Sn-Ag than for eutectic Pb-Sn under the same conditions. Although ample creep data on solders is available in the literature, the variety of microstructures and test conditions that prevail makes it difficult to correlate the data for reliability predictions.

Failure has been observed by the accumulation of both creep and fatigue damage in bulk solder samples [9,10]. At very low strain/stress ranges the material might exhibit minimal or no fatigue damage, whereas creep can occur at very low stresses as long as the temperature is high enough ($T>0.5T_m$) to provide the required thermal activation. The extent of creep depends upon the temperature and rate of application of stress/strain. Eutectic Pb-Sn solder subjected to cyclic loadings at 25^{0}C primarily deforms by creep processes [11]. As the frequency of loading is increased, it is seen that damage in the Pb-Sn solder due to creep in processes is suppressed and the failure occurs by fatigue [12, 13]. Thus it is not surprising that failure occurs through the interaction of

creep and fatigue as the solder joint experiences cyclic loading at temperatures well above $0.5T_m$.

Thermomechanical Fatigue Behavior of Solders

Fatigue is a measure of resistance to failure under cyclic loading. It can be classified as isothermal or 'thermal'. In isothermal fatigue, cyclic displacement occurs at a constant temperature, whereas in thermal fatigue, cyclic displacement occurs due to change in temperature when two materials with dissimilar coefficient of thermal expansion are joined. Fatigue can again be classified into high-cycle fatigue and low-cycle fatigue. Engineers are commonly used to designing for high-cycle fatigue when the part is subjected to relatively low loads. The elastic strains are much greater than the plastic strains in such conditions. Fatigue failure typically occurs after about 10^4 cycles and it is a stress-dominated event. Vibrational loads in the microelectronic packages generally cause high-cycle fatigue failures.

On the other hand, low-cycle fatigue occurs at higher loads where the plastic component of the strain is comparable to or even greater than the elastic strain. The temperature and power cycling are the primary causes of the low-cycle fatigue failures in microelectronic packages. Low-cycle fatigue is characterized as a strain-dominated event rather than a stress-dominated event [14]. Low-cycle fatigue in solder joints is termed as themomechanical fatigue (TMF) as solder joint is experiencing both change in temperature as well and a

change in the mechanical strain imposed by the coefficient of thermal expansion mismatch. Fatigue in the solder joints can be regarded as a high temperature low cycle fatigue phenomenon [15].

Unlike classical low-cycle fatigue, solder joints experience long hold times at each stress extreme, and these two extremes are at significantly different temperatures, as illustrated in **Figure 2** [16]. With each temperature change the solder joint is strained fairly rapidly to a new shape due to plastic deformation at strain rate between $10^{-4}$to 1 s^{-1} [16]. Once the thermal transients are settled, strain is relieved by stress relaxation in the joint. TMF is sensitive to changes in temperature as well as the duration of the dwell at the given temperature. For example, it is estimated that at temperatures greater than 80^{0}C, stress relaxation in bulk Pb-Sn solder will be complete in one minute whereas below -55^{0}C its extent over a period of days will be small [17]. If the unrelaxed stresses remaining in the cold part of the cycle are high enough they may cause a crack to propagate, and the stress might be relieved by fracturing processes similar to those of fatigue. Hence solder joints subjected to extreme temperature dwells are likely to fail by accumulation of damage due to creep (through relaxation) and fatigue processes.

Solder joint life prediction using the TMF data is carried out either by accelerated testing or by using the finite element model [6]. However, several subtleties are involved in the determination of acceleration factor. The

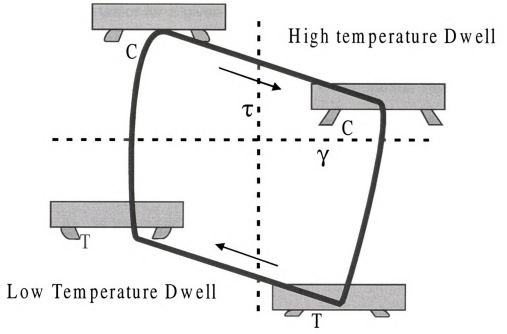

Figure 2.Low-cycle fatigue experienced by the solder joints under thermal cycling. Adapted from [16].

acceleration factor for a given test depends upon the temperature range and the cycling frequency. Also the microstructrural changes associated with accelerated testing may affect the extrapolation. The Coffin-Mason relationship commonly used to evaluate the low cycle fatigue is given by,

$$\Delta\gamma_p N_f{}^{\alpha} = \theta .$$

Where, $\Delta\gamma_p$ is the cyclic plastic shear strain range, N_f is the number of cycles to failure, α is the Coffin-Mason exponent and θ is a constant.

Typical values of α for eutectic Sn-Pb solders are 0.4-0.6 [6]. Lawson [18] carried out fatigue testes on Pb-rich solders and found out that hold periods at the tensile strain limits are damaging to the fatigue life of solder, although creep cavitation was not produced during the dwells. It was also observed that continuous cycling between 25 and 80^{0}C results in a shorter life than isothermal fatigue at 80^{0}C although this difference tends to disappear at high rates of deformation. Post-TMF test measurements indicate that strength of a joint as determined by a torque test, decreases as the number of cycles increases [19,20].

Strain rate may have a profound effect on the load strain hysteresis loop [21] as shown in **Figure 3.** In particular, peak tensile loads and the extent of

stress relaxation are markedly reduced at slow deformation rates [17]. Wild carried out comprehensive fatigue studies on shear lap specimens of eutectic

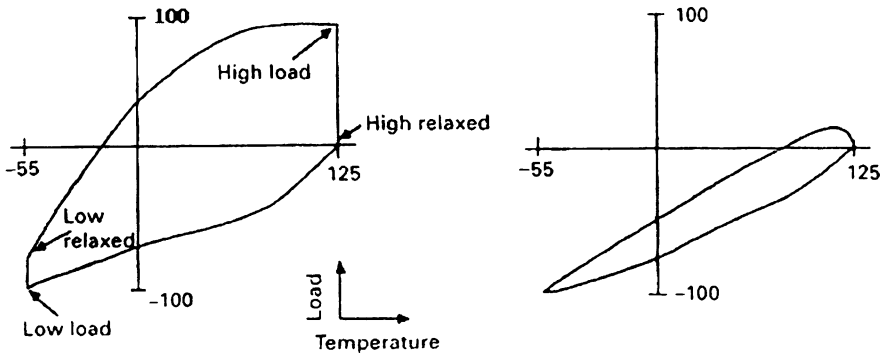

(a) (b)

Figure 3. Effect of strain-rate on the hysteresis loop for (a) fast deformation rate of 5.5 x 10^4/s and (b) slower deformation rate of 1.4 x 10^4/s for a near eutectic Pb-Sn alloy. Adapted from [21].

Pb-Sn alloy [14]. He observed a straight-line relationship between total shear strain range and cycles to failure on a logarithmic scale as shown in **Figure 4**.

There are significant concerns in experimental reliability testing of solder joints because of the uncertainty and variabilities in the mechanical properties of the solder and the substrate, the thermal stresses and the strains generated. Selection of appropriate testing parameters requires careful consideration. For example, test frequencies that are too high can produce results that are unrepresentative of the functional service as the dwell time may be too low to allow for stress relaxation. The types of specimens selected for TMF studies are either the actual components or the geometrically simplified test specimens, each having it's own advantages and disadvantages. With the former the problem is accurately determining the magnitude of thermal stresses and strain generated during testing. The problems with the complex stress strain distribution may be alleviated using simple joint geometries. While this also permits monitoring of damage under realistic conditions, determination of mechanical properties is not possible and interrupted testing is necessary [3]. In addition to the wide range of test types and specimen geometries, a further issue which impairs comparability of data from different sources is the definition employed to denote failure. Variations in the number of cycles to failure of an order of magnitude and changes in slope of Coffin-Mason plots may occur depending upon the parameter selected to define failure [3]. Failure criteria utilized include onset of a

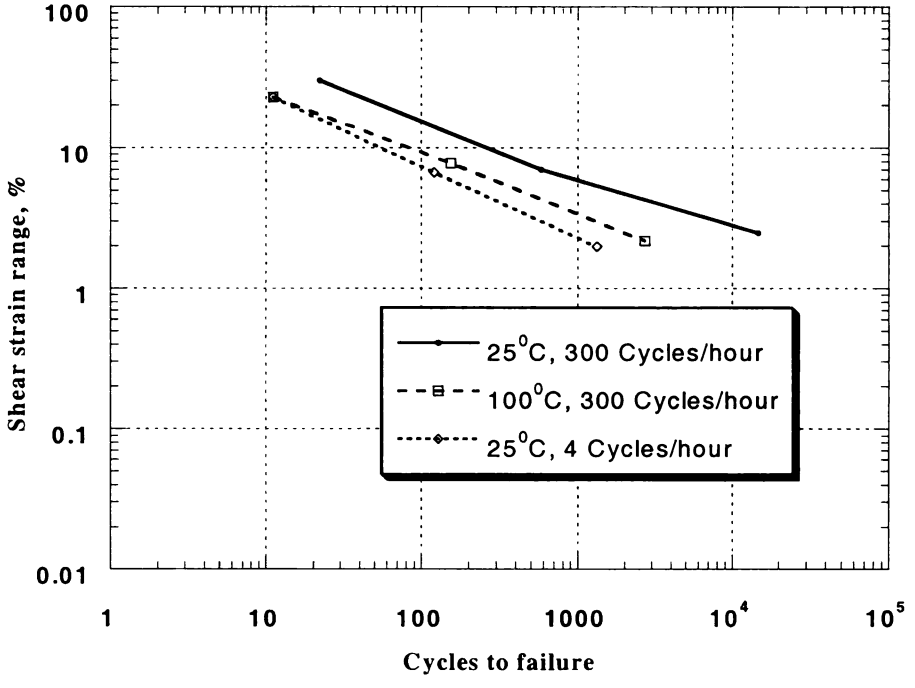

Figure 4. Lap shear fatigue test data for eutectic Pb-Sn alloy. Adapted from [14].

visible crack, the start of a stress drop or reaching a given percentage drop in stress, the ratio of maximum to minimum stress range, and change in electrical resistance. Under cyclic shear, crack growth is principally a function of applied plastic shear strain range and is unaffected by crack length [22]. This is in contrast to tension-compression fatigue in which the crack growth rate increases with crack length [3]. An important practical repercussion of this is a strong specimen size effect under shear-cycling as the crack growth must be longer to cause failure in tensile specimens. Consequently, the measured fatigue life of a laboratory test piece will be greater then that of a joint under otherwise similar conditions.

Stress relaxation in solders

Stress relaxation is time dependent deformation of a material under constant constraint (total strain). The stress relaxation test consists of deforming the sample to a predetermined displacement and holding it constant. The load drop exhibited is then subsequently recorded as a function of time. The load drops with time as the elastic strain within the sample and the machine is accommodated as the plastic strain within the sample. Although the total strain is constant during the stress relaxation experiment the material undergoes plastic deformation. This is due to the decrease in the elastic strain developed in the material prior to stress relaxation at the expense of increase in the inelastic strain (time dependent plastic strain).

Stress relaxation can also be studied using a test known as 'impression stress relaxation test'. In this test a cylindrical punch is used to indent the specimen. The punch is stopped after it reaches a certain depth and the load drop with time is recorded [23].

Stress relaxation test can be used to calculate the internal stress within a material. One of the methods of the measurement of the internal stress is the stress reduction technique [24]. In this method, the applied stress is suddenly reduced during a tensile test and a stress relaxation test is performed from the reduced stress level. If the reduced stress level is below the internal stress then internal stress reloading is observed and if the reduced stress is above the internal stress then the unloading occurs. The internal stress is taken as the stress at which the unloading rate is zero immediately following the stress reduction. Another approach to determine internal stress is to perform the stress relaxation test without load reduction. The internal stress is taken as the stress level at which the unloading rate goes to zero. The former technique is generally preferred as the internal stress can change during the stress relaxation because of microstructure evolution.

In actual industrial use, the solder joints are subjected to TMF. Dwell periods ranging from several hours to several days at the extreme temperature severely affect the fatigue life of the solder joints. The stress relaxation takes place during these dwell periods. As a result, nearly all the cyclic strains due to

coefficient of thermal expansion mismatch between substrate and the solder are converted to inelastic (permanent) strains. Hence with each cycle the fatigue damage is maximized. The effect of stress relaxation on the fatigue damage of the component during each strain cycle is qualitatively shown in **Figure 5** [25].

According to one school of thought, the area within the cyclic strain hysteresis loop is a qualitative measure of the fatigue damage the material has suffered. This damage is based on the assumption that the fatigue damage can be viewed as the progressive exhaustion of the ductility of the material and can be characterized by the inelastic work done during the cycle. Thus **Figure 5** represents the shorter fatigue life due to large hysterisis area. Time dependent behavior similar to this can be described as 'creep' (stress constant) or 'stress relaxation' (strain constant). In practice, neither of these exists in the pure from during the operation of the electronic device although stress relaxation tends to simulate these conditions more accurately. Thus stress relaxation is a close approximation of the conditions experienced by a solder joint during its operation.

Laboratory tests usually incorporate the dwells at the maximum strain limits since, for other structural alloys, dwells at intermediate levels have been shown to have a less marked effect on endurance [3]. Both eutectic and lead-rich solders have been found to be tensile-dwell sensitive i.e. a significant life debit is observed following fatigue with cycles containing dwells at maximum

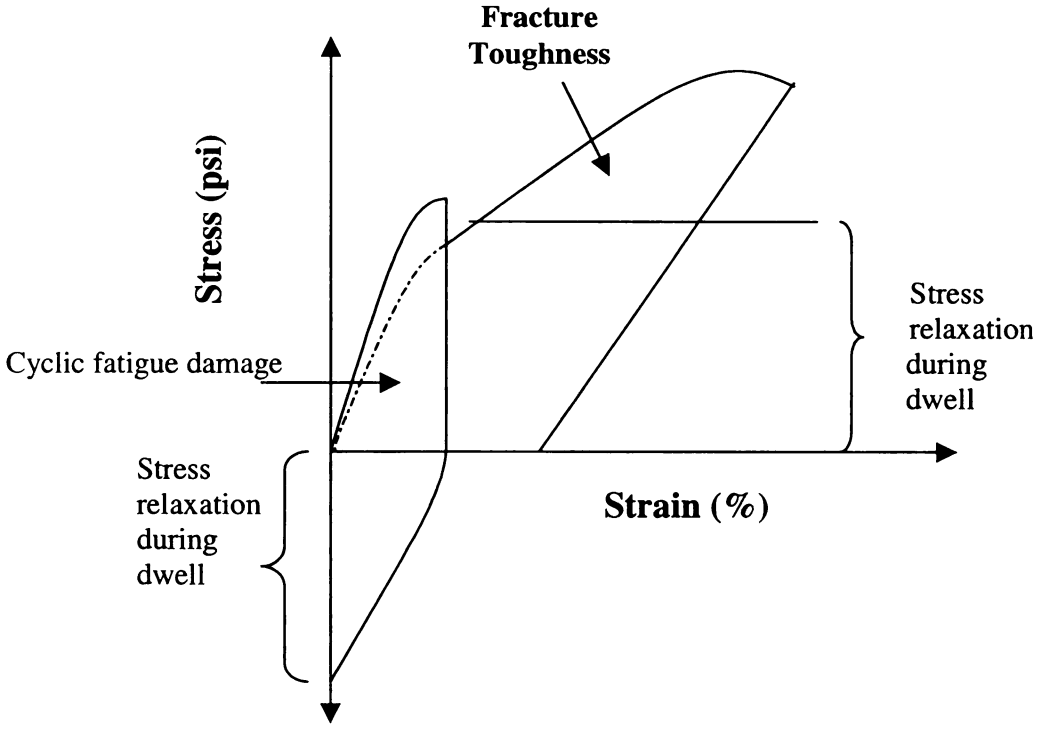

Figure 5. Effect of hysterisis loop on the cyclic fatigue damage. Figure shows stress-strain plot of a material which shows stress relaxation during fatigue. Adapted from [25].

tensile strain [10]. The reduction in endurance compared with that obtained for continuous cycling may be greater than an order of magnitude as shown **Figures 6** and **7** [10]. A saturation in this deleterious effect is observed when the dwell period exceeds about 100s [3]. Tests in vacuum on lead-rich solder [26] indicate that the nature of the time dependent damage accruing during the dwell is mechanical rather than environmental since number of cycles to failure is only slightly greater than in air.

Factors affecting the stress relaxation

The factors that affect the stress relaxation are obviously related to the temperature, cycle time and dwell time associated with a particular loading history. Strain rate and the strain imposed prior to stress relaxation also affect the stress drop during relaxation.

The microstructural processes that evolve during the stress relaxation in a solder joint are dependent upon the material composition, operating temperature and the strain rate. Microvoids and cracks have been found to nucleate and propagate along Sn-Sn and Sn-Sb phase boundaries during stress relaxation [27]. Studies on 60Pb-40Sn solder have been carried out to study the interactive effects of changing cyclic strain rate and changing temperature on the response of a leaded solder joint [28]. Frost and Howard [28] also examined TMF at two cycle frequencies, one high enough such that a quasi steady state microstructure was attained, and another low enough such that microstructure changed

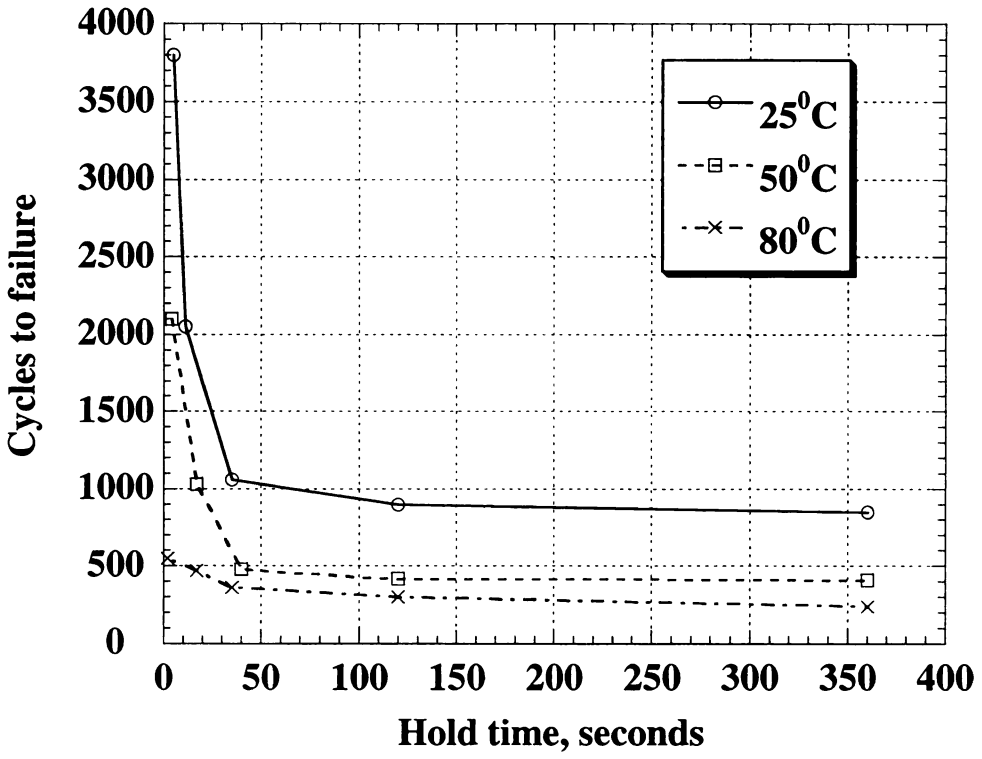

Figure 6. Effect of tensile hold time on the fatigue life of of a 96.5Pb–3.5Sn solder during strain controlled cycling. $\Delta\varepsilon_t$ (total strain range) is 0.6% and ramp time is 2.5 seconds. Adapted from [10].

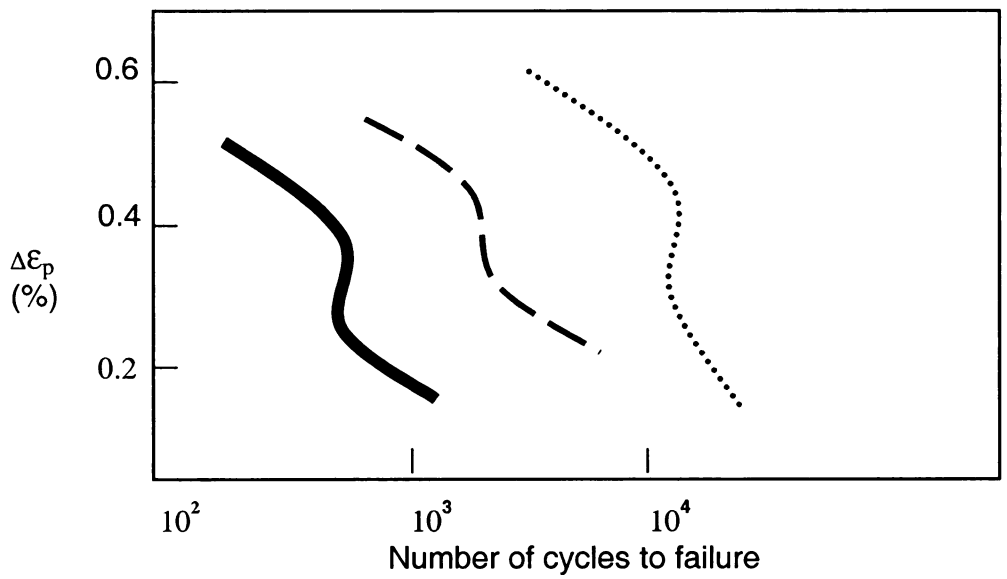

Figure 7. Effect of tensile dwell periods on endurance of a lead-rich solder at 25°C. ..... no hold; — — 30s hold; ▬▬ 360s hold. Adapted from [3].

cyclically with the strain. The effect of cyclic frequency on the fatigue life of the 60Sn-40Pb [29] as well as 96.5Pb-2.5Ag-Sn solder [30] has been investigated to show that decreasing cycle frequency results in the shorter fatigue lives for both the solders. This dependence was found to be stronger at 35^0C than at 150^0C. The mode of damage accumulation at higher strain rates (10^{-2}/sec) was primarily transgranular cracking while the cracking at lower strain rates was found to be mostly intergranular.

It has been observed [31] that the TMF damage in the Sn-Ag eutectic and 95.5Sn-4Ag-0.5Cu solders occurs by processes that are different from those observed in Pb-Sn solders. It was also found that apparently there was no grain coarsening in Sn-Ag solders as a consequence of thermal cycling.

Deformation mechanisms during relaxation

The components that are subjected to TMF at high homologous temperature (hot worked) can undergo a significant amount of stress relaxation due to inelastic strains [25]. These inelastic strains may result from mechanisms such as grain boundary sliding, grain boundary diffusion, dynamic recrystallization, intergranular crack growth, dislocation glide and dislocation climb.

Baker [32] performed compressive stress relaxation experiments on the chill cast 60Sn-40Pb solder and reported activation energy of 67 KJ/mole which

they concluded was independent of the stress level. They also found stress exponent n=3.4 for strain rates ranging from $7X10^{-8}$/s to 10^{-9}/s. Murty [33] demonstrated that stress relaxation test is complimentary to the differential strain rate test in the study of the superplastic behavior of the lead-tin solder. Kashyap and Murty [34] showed that prestraining the eutectic Sn-Pb sample before relaxation stabilizes the relaxation behavior. In their investigation of the eutectic Pb-Sn solder (grain size of 9.7-32 μm) they found n=1.7 and Q=44.5 KJ/mole at lower stress levels and n=11 and Q=100 KJ/mole at higher stress levels.

Rhode and Swerengen [35] reported a stress exponent of 5.7 at 25°C and 6.7 at 71°C. The stress exponent is considered to be independent of the temperature if only one deformation mechanism is rate controlling. The apparent change in the stress exponent with temperature suggests that two or more deformation mechanisms may be active during the stress relaxation experiments each having different contributions at different temperatures. Mukherjee and Arrowood's study [36] shows similar results. They obtained n= 2.08 in the stress range 1-6 MPa and n= 2.92 at higher stresses suggesting that different rate controlling processes are active during high and low stress regimes. Mavoori *et al.* [37] reported a stress exponent of 6 and activation energy of 33.5 KJ/mole for a bulk Sn-Ag solder. For Sn-Zn solder, they reported a stress exponent of 4.2 and activation energy of 106.9 KJ/mol. Cagnon et al. [38] have found out that in a Sn-Pb eutectic alloy at temperatures above or below –23°C different deformation mechanisms of inelastic deformation were dominant. It is most likely that

deformation mechanism does not change suddenly, but rather contributions of the glide controlled kinetics to the inelastic strain rate changes continuously with temperature. Other deformation mechanisms such as coble creep and grain boundary sliding were found unimportant for the stress relaxation. It has been generically determined through mechanical modeling that grain boundary sliding should account for only a small fraction of the total inelastic strain in a plastically deformed material and the stress dependence of the strain rate of the polycrystal is the same for the grain matrix for both high and low strain rates. Nix and Gibeling [39] determined that grain boundary sliding may be active in a material so long as grain boundary diffusion is also active. The reports of stress relaxation behavior of the Pb-Sn appear to vary widely. The variation stems from the different sample microstructures (cast structure vs. thermomechanically processed structure), alloy composition and stress- temperature regimes. These differences need to be better understood in order to select appropriate constitutive models for the prediction of deformation behavior of the solder joints.

Modeling of stress relaxation behavior

The stress drop in the relaxation process can be co-related to the plastic strain developed in the system, and it can be used to model the TMF behavior on the basis of Coffin-Mason relationship. Rhode and Swearingen [35] carried out stress relaxation experiments on four different solder alloys (63Sn-37Pb, 62.5Sn-37Pb-0.5Ag, 37.5Sn-37.5Pb-25In and 50Pb-50In). The microstructural aspects of deformation mechanisms were inferred by examining the magnitude of the

constitutive material parameters at –51°C, 25°C and 71°C. It was determined that thermally activated dislocation glide and recovery were the two deformation mechanisms contributing to the rate of inelastic deformation. In addition, the kinetics of dislocation glide was inferred to be a rate-controlling mechanism of deformation in Sn-Pb alloys only when the relaxation took place at –51°C, though it was not clear whether glide simply occurs with the same kinetics as recovery at the higher temperatures. The stress relaxation behavior was analyzed by fitting a power-law constitutive relation of the form:

$$\frac{d\sigma}{dt} = E\left(\frac{d\varepsilon_t}{dt} - \frac{d\varepsilon_p}{dt}\right).$$

$$\frac{d\varepsilon_p}{dt} = \varepsilon_0\left\{\frac{\sigma - \sigma_i}{\sigma_D}\right\}^m, \text{ and}$$

$$\sigma_D = \theta_0\left\{1 - \frac{C\sigma_D}{\frac{1}{\varepsilon_p^n}}\right\}\dot{\varepsilon}_p.$$

where ε_p is the inelastic strain, ε_t is the total strain, E is the Young's modulus, σ_D is the drag stress, σ_i is the back stress, θ_0 is the zero degree Kelvin strain hardening coefficient, C is the recovery coefficient and 'm' and 'n' are the material constants. The back stress was set to have a value of zero although non-zero values may be assigned so long as they depend only on the temperature.

A two term power-law model has been successfully employed by Hare and Stang [27] to characterize stress relaxation behavior of 63Sn-37Pb. They carried out the stress relaxation experiments at 25°C, 50°C, 75°C, 100°C and 125°C. The model contains two power-law terms to describe the high-stress behavior and low- stress behavior. The model is expressed by

$$\dot{\sigma} = -(A_1\sigma^{n1}\exp[\frac{-Q_1}{RT}] + A_2\sigma^{n2}\exp[\frac{-Q_2}{RT}]).$$

where A_1 and A_2 are the power-law constants, n_1 and n_2 are power-law stress exponents and Q_1 and Q_2 represent the apparent activation energy for the rate controlling mechanism of deformation, T is the temperature in degrees Kelvin, R is universal gas constant. They observed that the stress exponents and activation energies obtained for the cast and chilled specimens were markedly higher in the fine grain microstructure obtained by thermomechanical processing. This indicates that the rate controlling mechanism for these two microstructures are different. Towards the goal of incorporating creep and plasticity effects of solders into a comprehensive model, the unified creep plasticity model (McDowell model) has been proposed to predict the stress relaxation in solder joints [37].

Rationale for the present study

Stress relaxation data reported in the literature so far pertains to the bulk solder rather than the solder joint itself. In this project, an attempt was made to characterize the stress relaxation in the actual solder joint of realistic dimensions.

The stress relaxation in these two cases is different as stress drop during relaxation in the solder joint is limited by the constraints imposed on the joint. The role of constraints needs to be probed further. For example, the effect of stiffness of the constraint on the stress relaxation process needs to be studied.

Damage is sustained by the solder joint during the relaxation process occurring at dwell periods. The effect of damage sustained by the solder joint during relaxation process needs to be on the quantified in order to accurately model the TMF behavior of the solder joints. The effect of tensile dwell period versus compressive dwell period on the solder joint relaxation process is also an important parameter to be characterized. The question that needs further probing is whether stress relaxation is a stress dominated or a strain dominated event

EXPERIMENTAL PROCEDURE

Solder joint preparation

Half dogbone Cu specimens (0.5mm thick) formed by EDM (electro discharge machining) were covered with a solder mask such that approximately 1mm^2 area at the tip of the specimen was available for soldering. The specimens were cleaned using a solution of 50% nitric acid and water. α-L-200 flux was then applied to the specimens and the solder preform in form of a thin foil was placed at the tip of a half-dogbone specimen. This specimen with a solder foil on it was placed in the specially prepared aluminum fixture (**Figure 8**). Flux was applied to the tip of second half dogbone specimen and it was placed on the top of the first half dogbone Cu specimen. The assembly was then heated to 260^{0}C on a hot plate in approximately fifty seconds. At around 230^{0}C, the solder foils melted and joints were formed. The assembly was kept on the hot plate for about 5 seconds until the temperature reached 260^{0}C. Then the fixture was then removed from the hot plate and placed on an aluminum sheet to be cooled in air. The cooling rate during first minute was about 150^{0}C/min. It reached the room temperature in approximately 10 minutes. The soldered specimens were then removed from the fixture and the sides of these single shear lap joints were polished using standard metallography techniques for microstructural observation. The solder joints were polished using 240, 600 and 2000 grit sand papers in succession and then they were polished using 0.5 μm alumina polishing solution. The final polishing was carried out with slurry containing 0.1 μm SiO_2 particles. After polishing, the solder joints were observed under SEM for

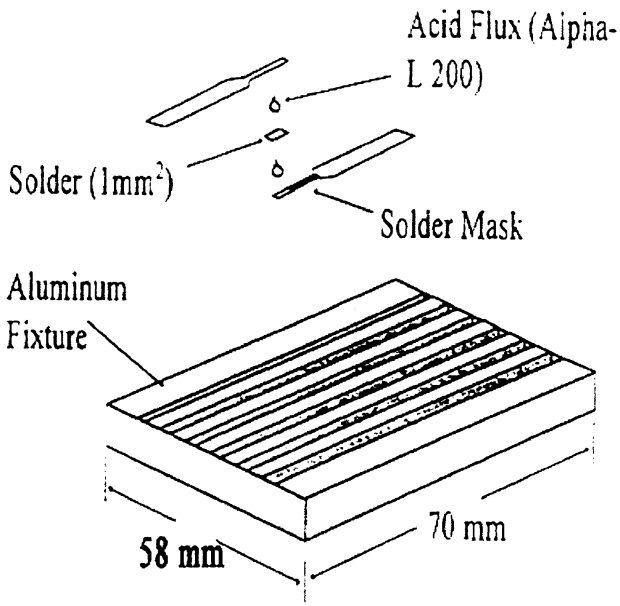

Figure 8. Single shear lap specimen assembly.

microstructural characterization and thickness measurement. The solder joints prepared were typically 100 μm thick. The above procedure was followed for preparing the eutectic Sn-Ag and composite solder (Sn-Ag solder containing 20 vol. percent of Cu_6Sn_5 introduced *in-situ* methods) joints. The typical solder joint obtained using the above procedure is shown in **Figure 9.**

Stress relaxation testing

Stress relaxation experiments were carried out on a tabletop screw driven universal tensile testing machine using a crosshead speed of 0.5 mm/min. The sample was loaded in the pneumatic grips to ensure that minimal torsional moment was applied to the specimen during the gripping process. The air pressure used for the grips was about 60 PSI. A miniature cylindrical furnace (about 1.25 inches in length and 0.75 inches diameter) was cut from a quartz tube. A heating element was wrapped around this furnace. The specimen was heated using this miniature furnace and the temperature variation was controlled within $\pm 1^{\circ}C$. The test set up was enclosed in sheets of Plexiglas to minimize temperature fluctuations due to air currents in the room. For high temperature relaxation tests, the furnace was switched on at least 2 hours before the start of the test to homogenize the temperature. Specially prepared insulating sheets were used to enclose the machine in order to maintain the Instron frame at a constant temperature (**Figures 10** and **11**).

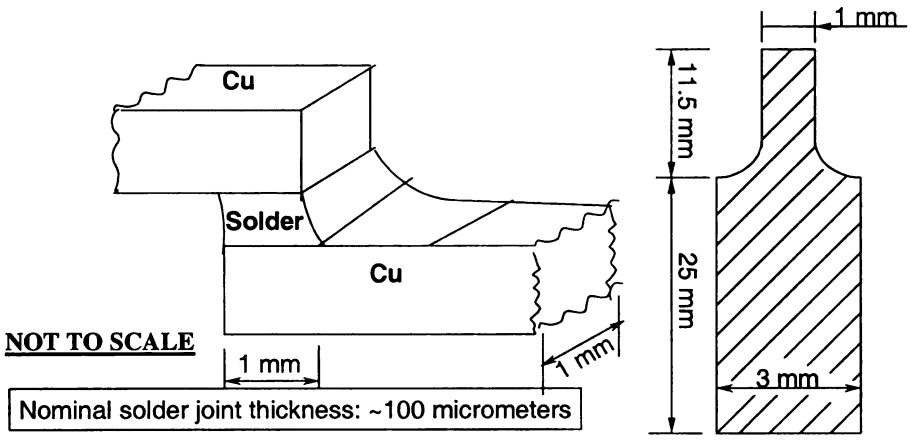

Figure 9. Schematic of typical single shear lap solder joint dimensions.

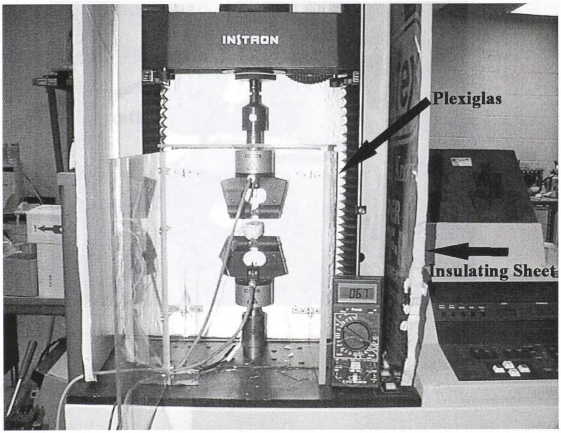

Figure 10. Stress relaxation experimental setup.

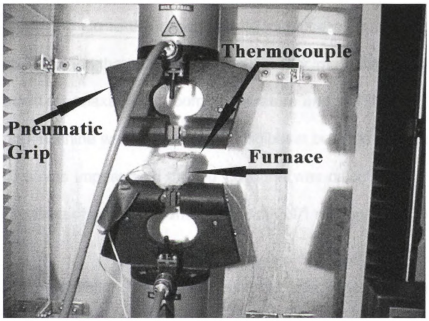

Figure 11. Stress Relaxation Experimental setup- a closeup view.

In this solder joint stress relaxation process, there is contribution of the machine and the Cu to the stress relaxation process. In order to evaluate the relaxation in Cu and the machine an identical specimen without the solder joint in it was tested for relaxation at room temperature and at 150^{0}C. The relaxation in Cu and the machine was found to be negligible at both the temperatures (**Figure 12**). The stress imposed on the Cu dogbone was calculated by assuming the rectangular area of cross section having width of 1 mm and thickness of 0.5 mm.

Stress relaxation tests were carried out after imposing different extents of displacements. Selected displacement values imposed stress states prior to relaxation corresponding to points A, B or C as shown schematically in **Figure 13**. Shear strains imposed prior to relaxation corresponding to points A, B and C were calculated by two methods. In one approach, plastic shear strain in the joint was obtained by extracting the plastic displacement value from the loading part of relaxation curve and dividing this value by the thickness of the solder joint (**Figure 14A)**. In the other approach, plastic shear strain values were calculated by directly measuring the displacement of the line pattern marked on the specimen (**Figure 14B**) and dividing it by the thickness of the solder joint. The line pattern was intentionally formed on the surface of the solder joint across the thickness as well as the length of the joint by using the excimer laser ablation technique. Details of this technique can be found elsewhere [40].

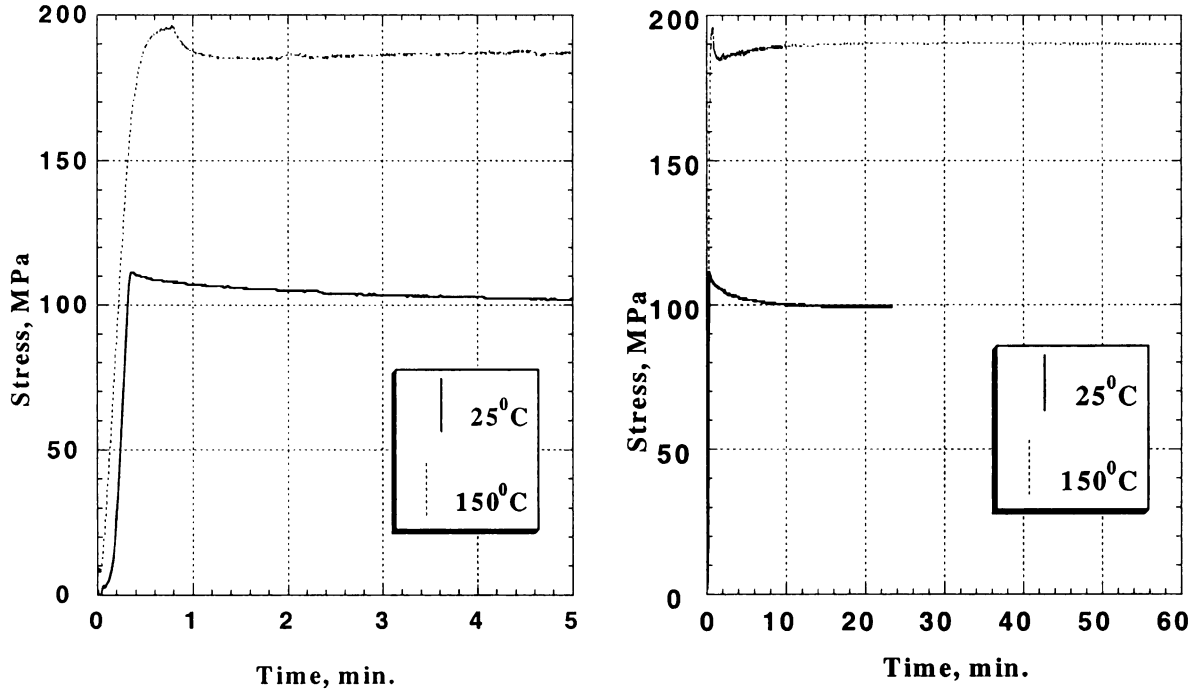

Figure 12. Stress relaxation of Cu dogbone at 25°C and 150°C without the solder in it. Figure shows (a) relaxation in the first 5 minutes and (b) relaxation in 1 hour.

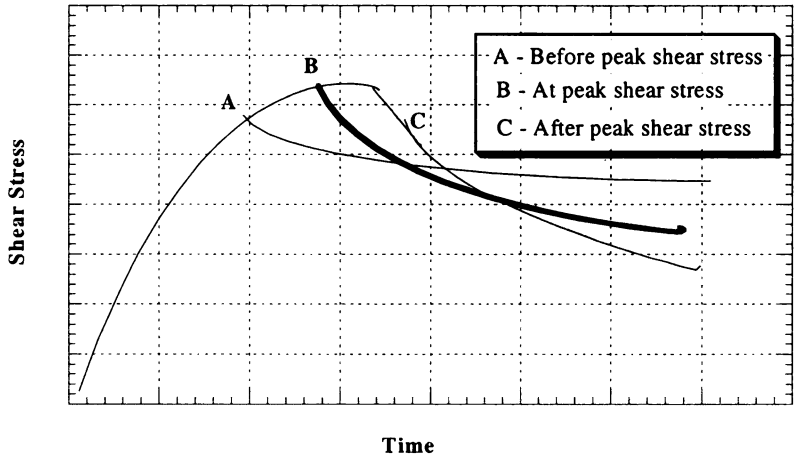

Figure 13. Schematic illustration of the points representing the stress level imposed prior to the beginning of relaxation and the typical relaxation behavior observed under such condition.

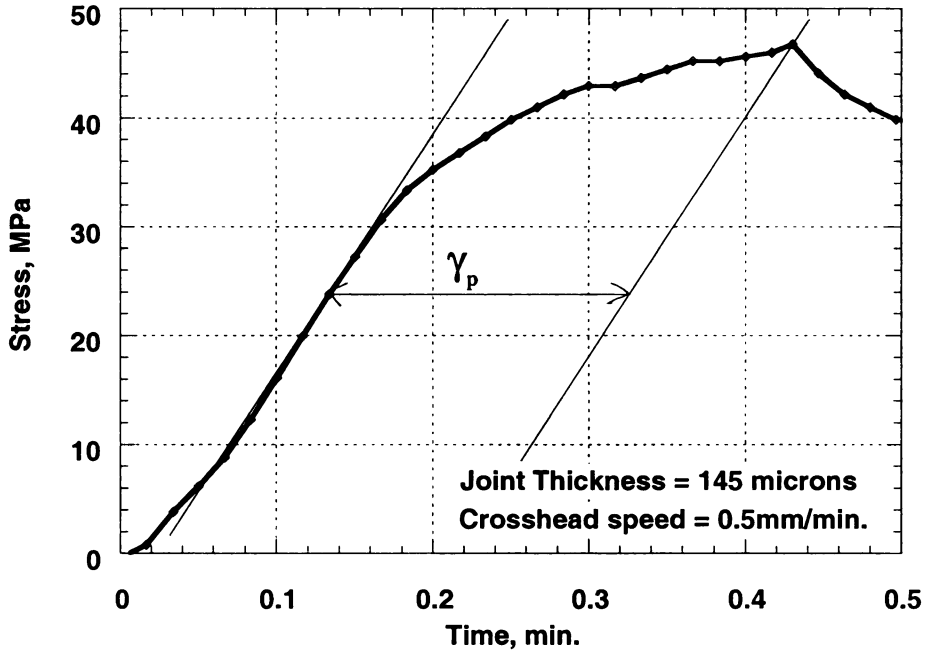

Figure14A. Measurement of the plastic shear strain imposed prior to the start of relaxation for a eutectic solder joint at 25°C. Magnitude of plastic shear strain is computed based upon the time interval between points X and Y using the crosshead speed of 0.5mm/min. and joint thickness of 145 μm.

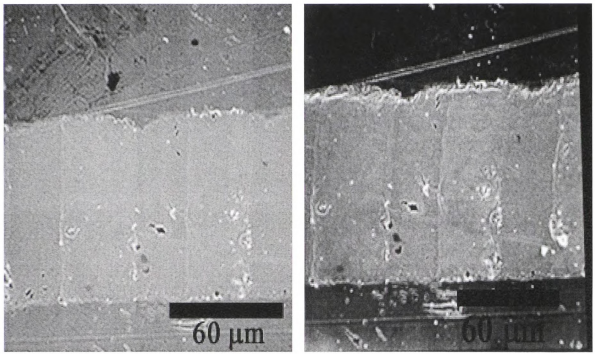

(a) (b)

Figure 14B. Measurement of the plastic shear strain in the solder joint tracing the deformation of laser ablation pattern. Figure shows laser ablation pattern of a eutectic Sn-Ag solder joint at 25°C. Figure shows line pattern (a) before relaxation and (b) after relaxing for 1 hour.

At the end of the test the data collection was stopped and then the specimen was removed from the grips for microstructural characterization. The relaxation process was repeated up to 3 times. The specimen was then reloaded into the tensile testing machine and was broken into two halves. The broken Cu dogbone halves were examined in the SEM to find the true solder area after excluding the area of porosity. The load values obtained from the relaxation test were then converted to stress values by using the true solder area.

RESULTS AND DISCUSSION

This discussion compares the stress relaxation behavior in solder joints with and without prior deformation history at 25°C and 150°C. The effect of constraints on the % stress drop obtained during relaxation, comparison of the relaxation behavior of the bulk tensile specimens with the actual solder joints tested in shear, the derivation of the shear creep rate from the relaxation data and the possible role of the recovery processes in stress relaxation are the issues that are discussed here.

Comparison of the plastic shear strain values obtained by mapping the movement of the laser pattern on the surface of the relaxed solder joint with the plastic shear strain values obtained from the loading part of the relaxation curve is shown in **Table 5**. Shear strain values calculated by using these two methods were found be similar.

In order to assess the relaxation behavior of solder joints without any prior deformation history, relaxation experiments were carried out at 25°C on 3 similar composite Sn-Ag solder joints (with similar thickness) by imposing different extents of shear displacements corresponding to points A, B and C as shown in **Figure 15a** (the arrows in the figure indicate where the crosshead displacement stopped). The results from these experiments indicate that the % stress drop during relaxation is dependent upon the plastic strain imposed prior to relaxation.

Table 5. Comparison of shear strain values obtained by mapping the movement of the laser pattern on the microstructure of the relaxed solder joint and shear strain obtained from the loading part of relaxation curve.

Shear strain (laser pattern)	Shear strain (plot)
0.303	0.346
0.08	0.1
0.6678	0.69
0.23	0.27

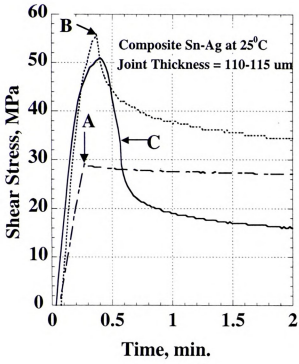

(a)

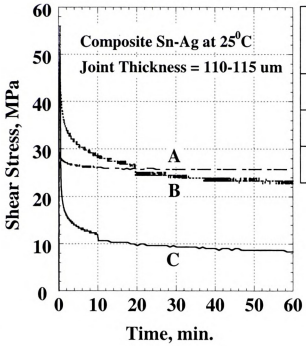

(b)

Relaxation	Plastic Shear Strain	% Stress Drop in 1 Hour
A	0.08	10
B	0.48	53
C	1.5	77

Figure 15. Stress relaxation curves of 3 different composite solder joints of thickness around 110-115 μm tested at 25°C. Figure shows (a) stress drop in the first 2 minutes. Arrows indicate the beginning of stress relaxation. (b) Stress drop in 1 hour. Crosshead speed = 0.5 mm/min. and joint thickness = 110-115 μm.

A greater imposed plastic shear strain before relaxation causes a greater % stress drop during relaxation.

Figure 16 shows stress relaxation behavior for 3 sequential load-relaxation experiments on a composite Sn-Ag joint at 25°C. Curve A in **Figure 16** shows that the stress drop in one hour is about 37 %. The same sample was unloaded, reloaded and stress relaxation experiments were subsequently carried out for loading conditions B and C in that order. It can be seen that under these conditions the stress drop in 1 hour is about 53 % and 63 % respectively. The eutectic solder joint in **Figure 17** also shows similar trends. The relaxation behavior for 3 sequential loading events is similar to the relaxation behavior of specimens without prior deformation history.

Sequential stress relaxation experiments were carried out on the eutectic and the composite solder joints at 150°C. The stress relaxation curve of a eutectic and composite Sn-Ag solder joint subjected to 2 sequential stress relaxation experiments at 150°C is shown in **Figures 18 and 19**. Comparing relaxation at 150°C with room temperature relaxation (**Figures 16 and 17**) it is seen that the % stress drop at 150°C is greater than the % stress drop at room temperature for similar values of imposed plastic shear strain. Magnitude of plastic shear strain required to achieve a given % of stress drop is considerably smaller at 150°C than at 25°C for eutectic and composite Sn-Ag solder joints.

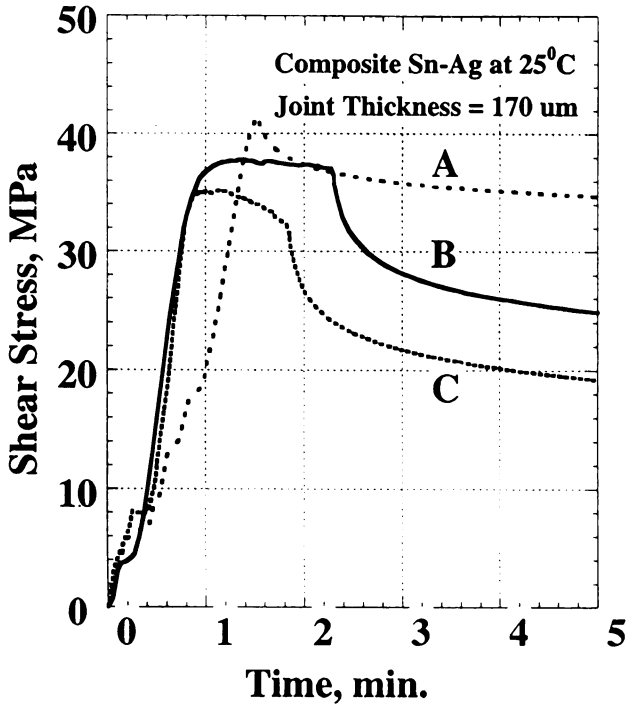

(a)

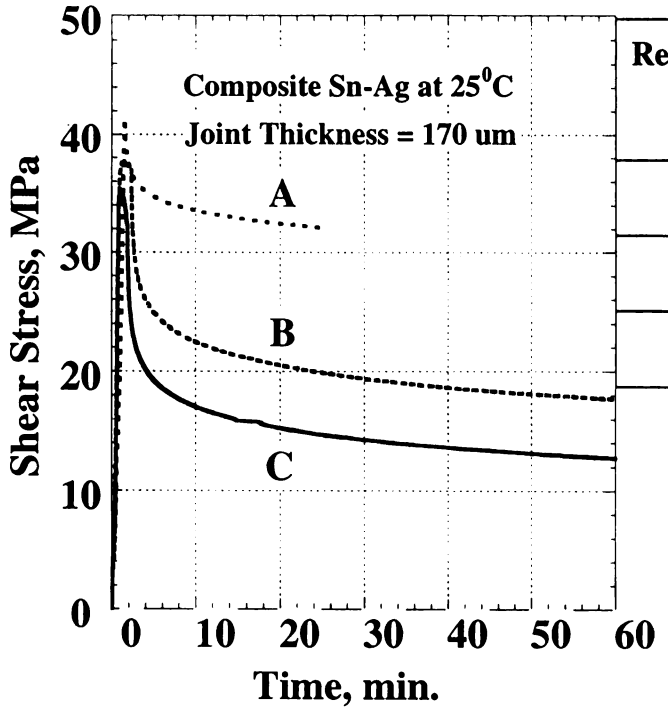

(b)

Relaxation	Plastic Shear Strain	% Stress Drop in 1 Hour
A	0.3	37
B	0.6	53
C	0.7	63

Figure 16. Stress relaxation curves for a composite Sn-Ag solder joint subjected to sequential stress relaxation experiments at 25°C. Figure shows (a) stress drop in the first 5 minutes and (b) stress drop for the same sample in 1 hour. Crosshead speed = 0.1mm/min and joint thickness = 170 μm.

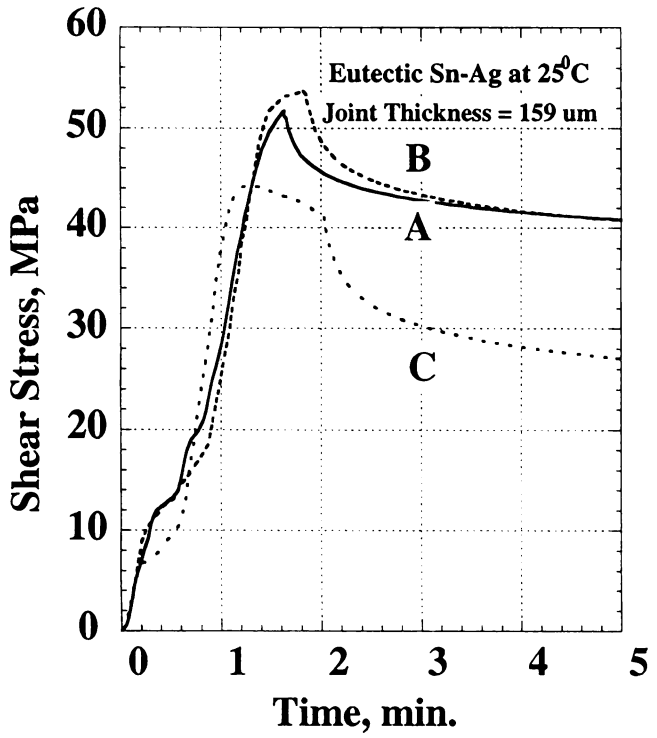

(a)

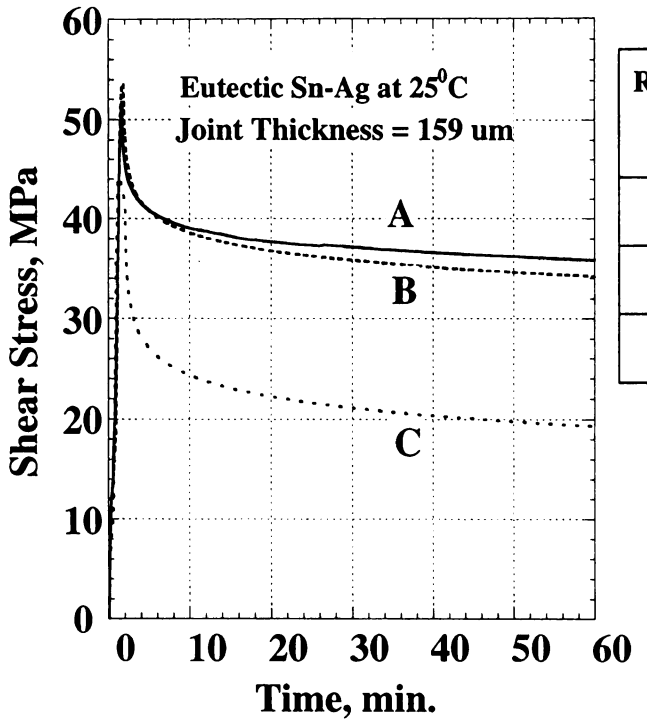

(b)

Relaxation	Plastic Shear Strain	% Stress Drop in 1 Hour
A	0.25	31
B	0.26	35
C	0.63	57

Figure 17.Stress relaxation curves for a eutectic Sn-Ag solder joint subjected to sequential stress relaxation experiments at 25°C. Figure shows (a) stress drop in the first 5 minutes and (b) stress drop for the same sample in 1 hour.
Crosshead speed = 0.1 mm/min and joint thickness = 159 μm.

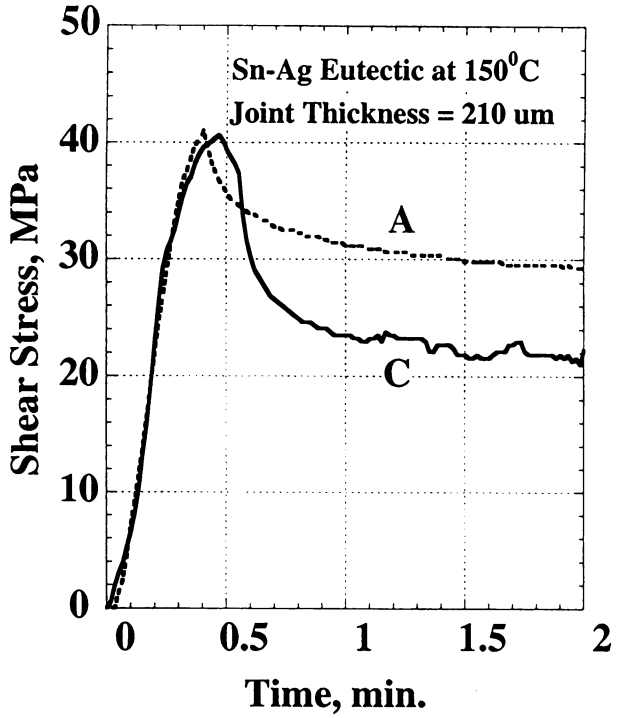

(a)

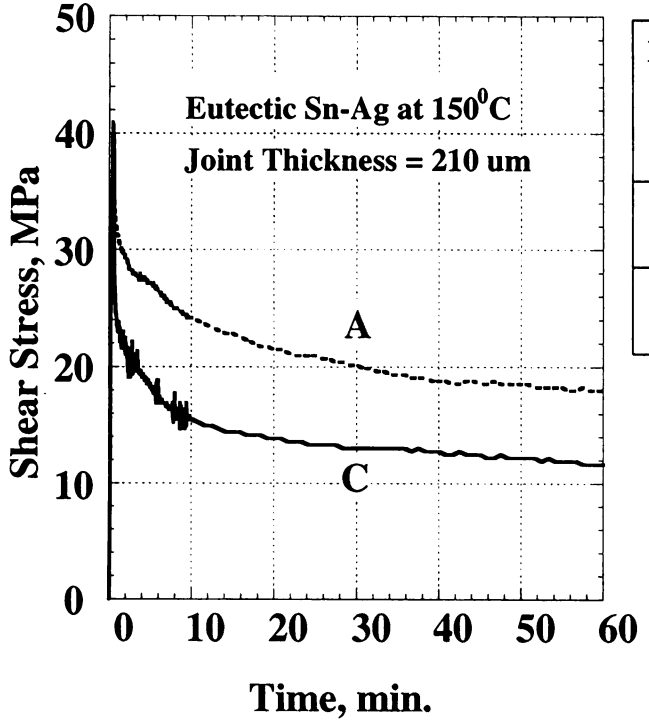

(b)

Relaxation	Plastic Shear Strain	% Stress Drop in 1 Hour
A	0.2	56
C	0.67	70

Figure 18. Stress relaxation behavior of eutectic Sn-Ag solder joint subjected to sequential relaxation tests at 150°C. Figure (a) shows stress drop in the first 2 minutes and (b) shows stress drop for the same sample in 1 hour. Crosshead speed = 0.5mm/min and joint thickness = 210 μm.

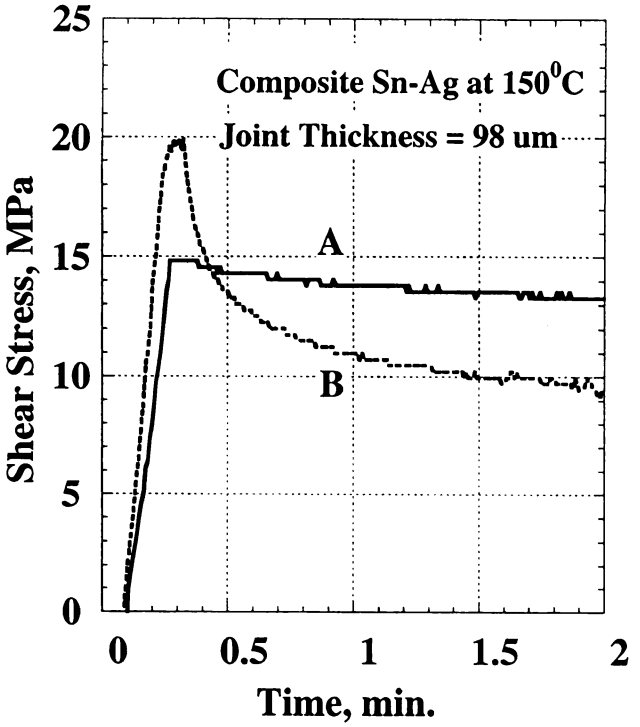

(a)

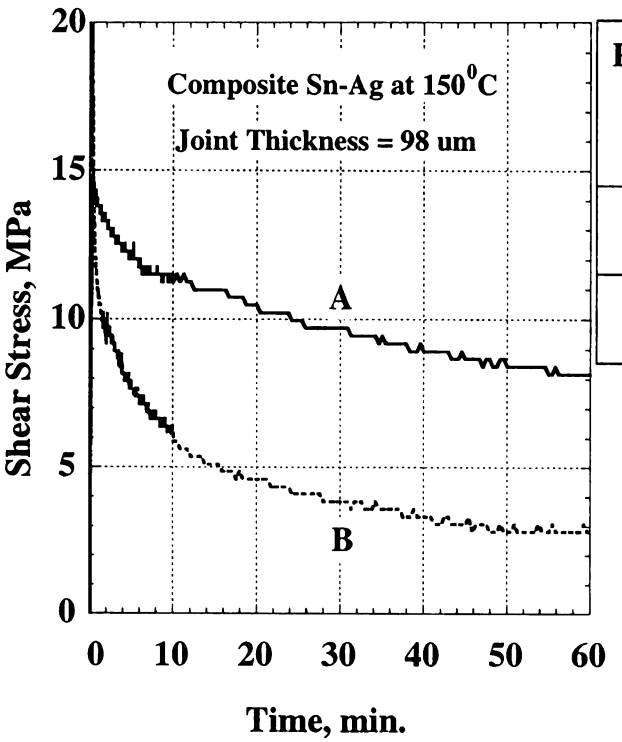

(b)

Relaxation	Plastic Shear Strain	% Stress Drop in 1 Hour
A	0.05	37
B	0.4	71

Figure 19. Stress relaxation of a composite Sn-Ag solder joint subjected to sequential relaxation tests at 150°C. Figure shows (a) stress drop in the first 2 minutes of relaxation and (b) stress drop in 1 hour. Crosshead speed =0.5mm/min and joint thickness = 98 μm.

The trends in these plots indicate that for both eutectic Sn-Ag as well as composite solder joints the % stress drop obtained in relaxation increases with increasing plastic shear strain imposed prior to the relaxation process. The % stress drop obtained when the solder joint starts relaxing before reaching the maximum shear stress is smaller than the condition where the solder joint begins to relax at strains beyond the maximum shear stress.

Figures 20 and 21 show that the % stress drop during relaxation increases with increasing imposed plastic shear strain for both the alloys at 25^{0}C and 150^{0}C. The % stress drop observed during relaxation at 25^{0}C increases rapidly with increasing plastic shear strain at lower values of imposed plastic shear strain. At higher values of imposed plastic shear strain (above 0.5) the change in % stress drop appears to be less dramatic for both the alloys. For relaxation at 150^{0}C, the % stress drop in 1 hour is higher than the stress drop at 25^{0}C for a similar value of imposed plastic shear strain. This applies to both eutectic as well as composite solder joint.

Effect of deformation history

It is important to study the effect of accumulated plastic shear strain in the solder joints subjected to sequential load relaxation experiments because repeated reloading of solder joints occurs during the thermomechanical fatigue.

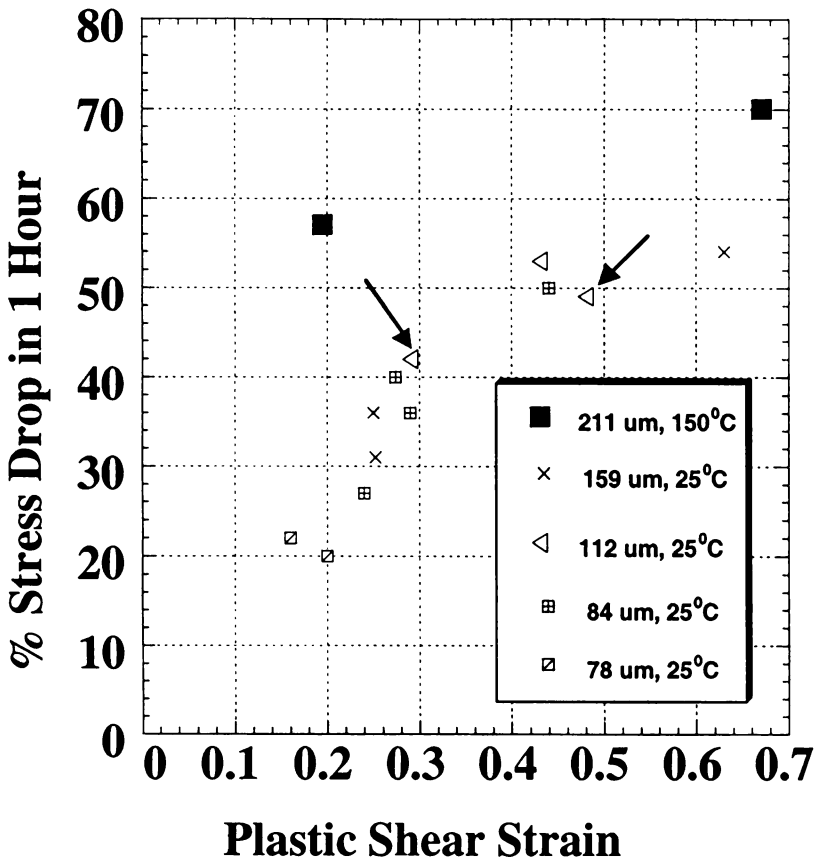

Thickness (μm)	Plastic Shear Strain	Stress Drop in 1 Hour (%)
211 (150°C)	First – 0.195	57
	Second – 0.67	70
159(25°C)	First – 0.25	31
	Second – 0.26	36
	Third - 0.63	54
112(25°C)	First –0.48	49
	Second – 0.43	53
	Third - 0.29	42
84(25°C)	First – 0.24	27
	Second – 0.29	36
	Third - 0.27	40
	Fourth - 0.44	50
78 (25°C)	First - 0.20	20
	Second – 0.16	22

Figure 20. Correlation between magnitude of plastic shear strain imposed prior to relaxation and % stress drop during relaxation in eutectic Sn-Ag solder joints of different thickness values subjected to sequential relaxation experiments. Adjacent table shows the sequence in which the experiments were carried out.

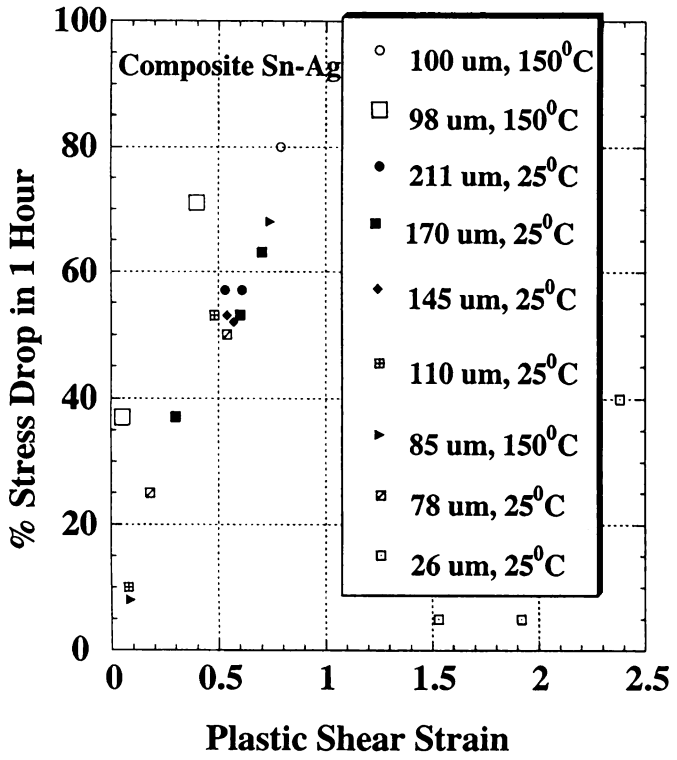

Thickness (μm)	Plastic Shear Strain	Stress Drop in 1 Hour (%)
98 (150°C)	First – 0.05	37
	Second – 0.4	71
100 (150°C)	First – 0.79	80
211 (25°C)	First – 0.61	57
	Second - 0.53	57
170(25°C)	First –0.3	37
	Second – 0.6	53
	Third - 0.7	63
145(25°C)	First – 0.57	52
	Second – 0.54	53
110 (25°C)	First - 0 .08	10
	Second - 0.48	53
85 (25°C)	First - 0.085	8
	Second - 0.74	68
78 (25°C)	First - 0.18	25
	Second - 0 .54	50
26 (25°C)	First – 1.92	5
	Second –1.53	5
	Third – 2.38	40

Figure 21. Correlation between magnitude of plastic shear strain imposed prior to relaxation and % stress drop during relaxation in eutectic Sn-Ag solder joints of different thicknesses subjected to sequential relaxation experiments. Adjacent table shows the sequence in which the experiments were carried out.

For the 112 μm thick eutectic solder joint in **Figure 20**, the % stress drop observed with a strain of 0.29 during the third relaxation experiment (but with a large cumulative plastic shear strain of 1.2) is lower than the % stress drop obtained during the first relaxation experiment (with a plastic shear strain of 0.48 - see arrows and table in **Figure 20**). This trend indicates that when a eutectic Sn-Ag solder joint is subjected to sequential stress relaxations that includes unloading, the % stress drop observed appears to be independent of the plastic shear strain accumulated in previous relaxation events. The plastic shear strain imposed immediately prior to relaxation determines the magnitude of stress relaxation. The same phenomenon can be seen in the 211 μm composite Sn-Ag solder in **Figure 21** where a similar prestrain causes a smaller % of relaxation. This phenomenon may be explained on the basis of recovery that occurs over time when the specimen was unloaded from the stress relaxation apparatus and examined for microstructural characterization, which generally occurred over a period of 2-5 hours.

Although the magnitude of stress relaxation is largely determined by the shear strain imposed immediately prior to relaxation, there is some effect of the deformation history. For the 159 μm thick eutectic joint in **Figure 20**, the % stress drop at 25°C in second relaxation (53 %) is slightly higher than % stress drop observed during the first relaxation (49%) in spite of a lower plastic shear strain imposed in the second relaxation as compared to first relaxation. This trend is also evident for the 112 μm eutectic specimen in **Figure 20** as well as 145 μm

and 211 μm composite the Sn-Ag in **Figure 21**. Thus there is a small but measurable secondary effect where greater relaxation occurs for larger cumulative strain when the same immediate prestrain is imposed.

Stress relaxation without unloading

In order to verify the effect of previous deformation history, another set of sequential stress relaxation experiments without unloading were carried out at 25^{0}C on eutectic Sn-Ag joints. From **Figures 22** and **23** the maximum shear stress reached during each relaxation event increases, and after the 4th relaxation there is a steady decrease in the maximum shear stress attained because of the microstructural changes within the specimen during the previous relaxation events. Although magnitude of plastic shear strain added during each relaxation is very small (ranging from 0.02-0.05) there is a steady increase in the % stress drop during each relaxation event because of the accumulated shear strain. After 3 prior relaxation events the % stress drop obtained is higher (about 40 % for accumulated shear strain of 0.15 as shown in **Figure 22**) as compared to the 20 % obtained in **Figure 20** for a similar values of shear strain. Comparatively higher % stress drop for a small value of imposed shear strain suggests that there is a significant effect of prior history on the relaxation behavior in the stress relaxation without unloading. **Figure 23** shows that after the relaxation involving a long hold time (about 700 minutes), the % stress drop obtained during next relaxation events increases dramatically indicating that the longer hold time had a large effect on the microstructure.

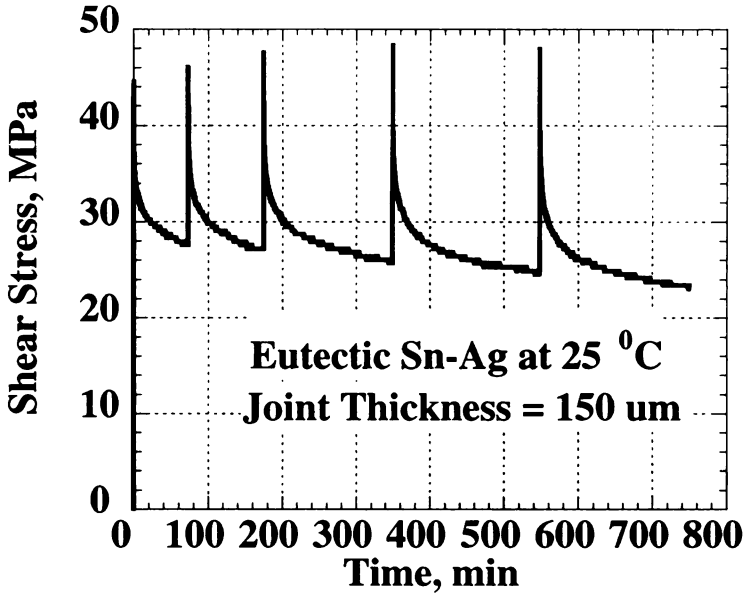

(a)

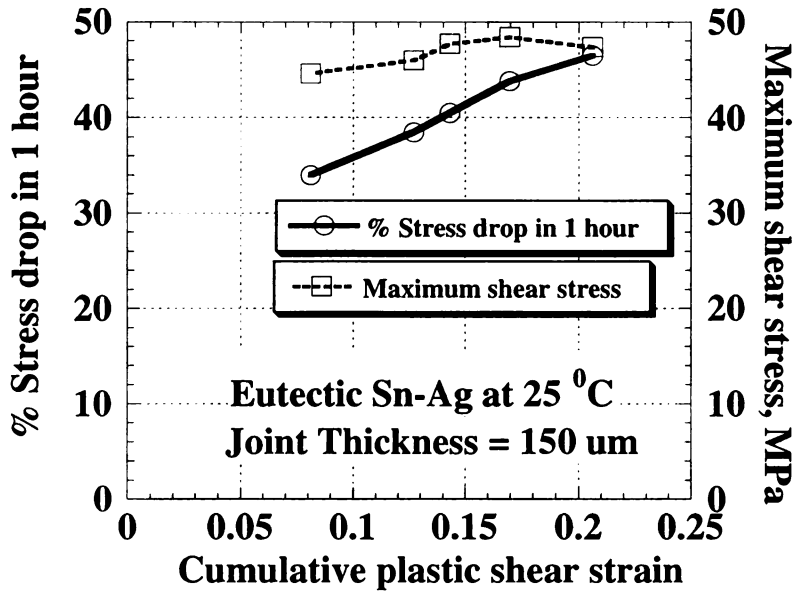

(b)

Figure 22. Sequential Stress relaxation without unloading in a eutectic Sn-Ag sample at 25°C. Figure (a) shows the stress relaxation and without unloading (b) shows the variation of maximum shear stress and % stress drop obtained during each relaxation. Joint thickness = 150 μm and crosshead speed = 0.5 mm/min.

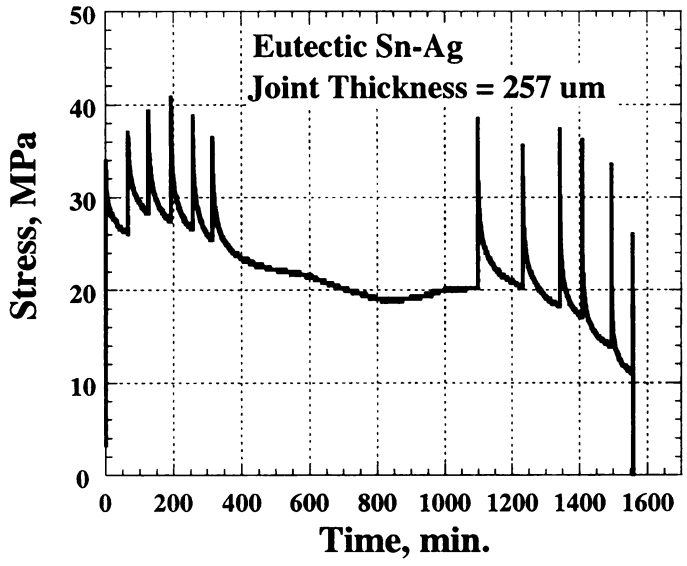

(a)

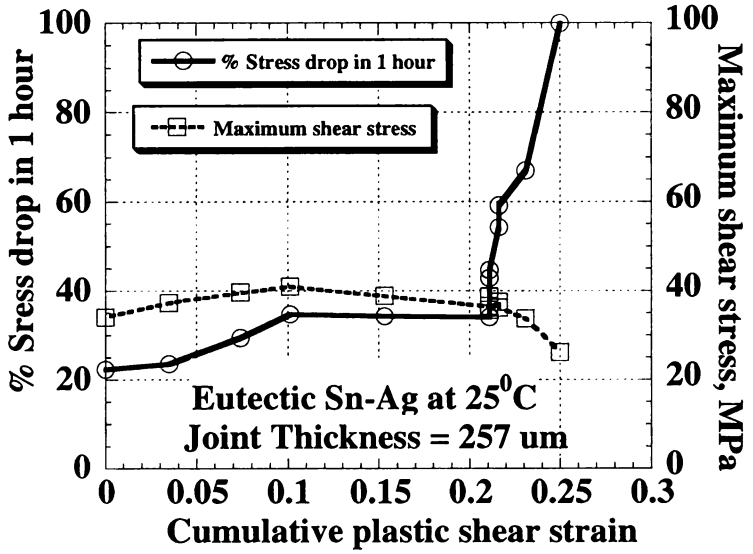

(b)

Figure 23. Stress relaxation of a eutectic Sn-Ag joint without unloading at 25°C. Figure (a) shows the sequential stress relaxation behavior and (b) shows the variation of maximum shear stress and % drop during each relaxation with cumulative plastic shear strain. Joint Thickness = 257 μm and crosshead speed= 0.5 mm/min.

Effect of Constraints

For very thin solder joints (less than 50 μm thick), imposed constraints significantly affect the magnitude of stress drop obtained during the relaxation process. This can be clearly seen in **Figure 21** for the 26 μm composite solder joint, where in spite of a very high value of imposed plastic shear strain, the stress drop achieved during relaxation in the first two experiments is very low (about 5%).

Comparison to stress relaxation behavior of bulk Specimens

In the studies conducted by Mavoori *et al.* [4] on Sn-Ag bulk solder specimens, tensile stresses relax to zero in less than 24 hours at 80°C. The specimens used in their studies were bulk tensile specimens having minimal constraints imposed on the radial deformation. The current study shows that eutectic solder joints (having single shear lap geometry) with large constraints imposed does not relax to zero stress at 150°C even after 20 hours (**Figure 24**) This indicates that the stress relaxation behavior of solder joints is dependent on the geometry of the specimen. It also underscores the fact that constraints play an important role in the solder joint stress relaxation process [3].

Mavoori *et al.* [4] have shown an important correlation between tensile stress relaxation tests and isothermal fatigue tests. They observed that with the increase in hold time the number of cycles to failure under fatigue decreases considerably. However, a hold time greater than 120s was not observed to cause a further decrease in cycles to failure during fatigue. They ascribed this behavior to almost complete relaxation of tensile stresses for a hold time of 120s and

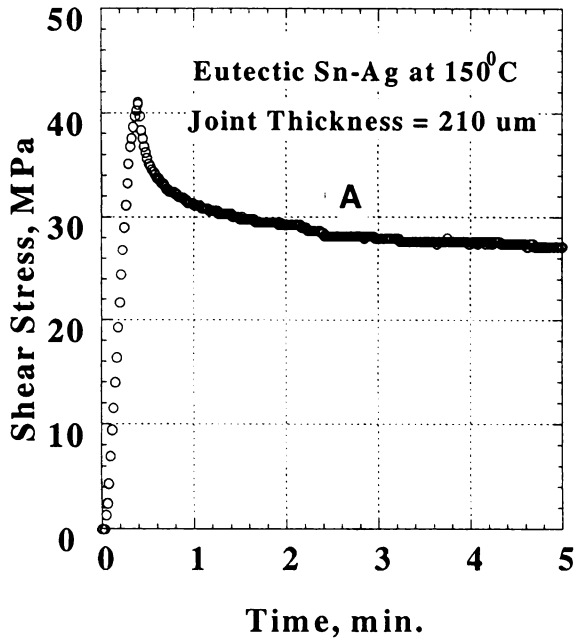

(a)

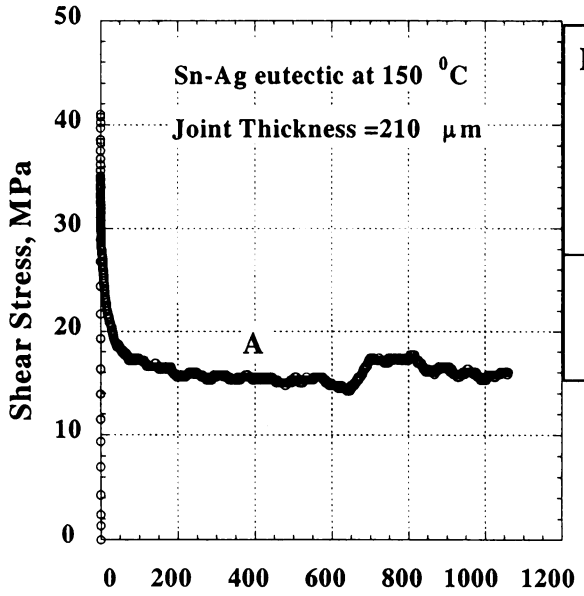

(b)

Relaxation	Plastic Shear Strain	% Stress Drop in 20 Hours
A	0.2	67

Figure 24. Stress relaxation of a eutectic Sn-Ag solder at 150°C showing that even after 150°C the stresses do not relax to zero. Figure (a) shows the stress drop in the first 5 minutes and (b) shows the stress drop in about 20 hours. Joint Thickness = 210 μm and crosshead speed = 0.5 mm/min.

above. It was suggested that during relaxation, damage accumulates in the sample with the formation of slip steps. Increasing relaxation time beyond 120s did not cause further damage since the tensile stresses were already relaxed to a low value. But the present data indicate that in shear loading the imposed constraints do not allow the complete relaxation and the shear stresses that remain in the joint may be enough to cause further damage during the hold period which may be considerably longer than 120s.

Determination of shear creep rate

In the stress relaxation test the total shear strain imposed prior to relaxation process is given by,

$$\gamma_t = \gamma_e + \gamma_p, \qquad (1)$$

where, γ_t is the total shear strain which is constant, γ_e is the plastic shear strain in the specimen and the machine and γ_p is the plastic shear strain in the specimen.

During stress relaxation, the total shear strain γ_t is held constant but the plastic shear strain γ_p in the sample increases at the expense of decrease in the elastic shear strain γ_e within the solder and the elastic strain in the machine.

The load drop during relaxation process can be described by starting with,

$$P = -K x, \qquad (2)$$

where, P is the load applied on the specimen, K is the combined stiffness of the specimen and the machine, and x is the displacement of the crosshead.

Taking time derivative of equation 2 we get,

$$\dot{x} = -\frac{\dot{P}}{K}, \qquad (3)$$

The value of 'K' was obtained by using the load-displacement data during the loading part of the curve obtained by testing of an identical specimen not containing the solder joint in it. 'K' was found to be 321 MN/m at room temperature and 271 MN/m at 150°C.

The instantaneous plastic shear strain rate in the specimen is given by

$$\dot{\gamma}_p = \frac{\dot{x}}{h}, \qquad (4)$$

where, h= thickness of the solder joint.

Combining equations 3 and 4,

$$\dot{\gamma}_p = -\frac{\dot{p}}{Kh}. \qquad (5)$$

This result is similar to the one obtained by Darveaux *et al.* [41]. The variation of $\log\dot{\gamma}_p$ vs. $\log\tau$ is plotted in **Figures 25** and **26**. The slope 'n' is the stress exponent in the empirical creep equation given as,

$$\dot{\gamma} = \tau^n \exp\left(\frac{-Q}{RT}\right),$$

where $\dot{\gamma}$ is the shear strain rate, τ is the shear stress, 'n' is the stress exponent, Q is the activation energy, R is the universal gas constant and T is the absolute temperature.

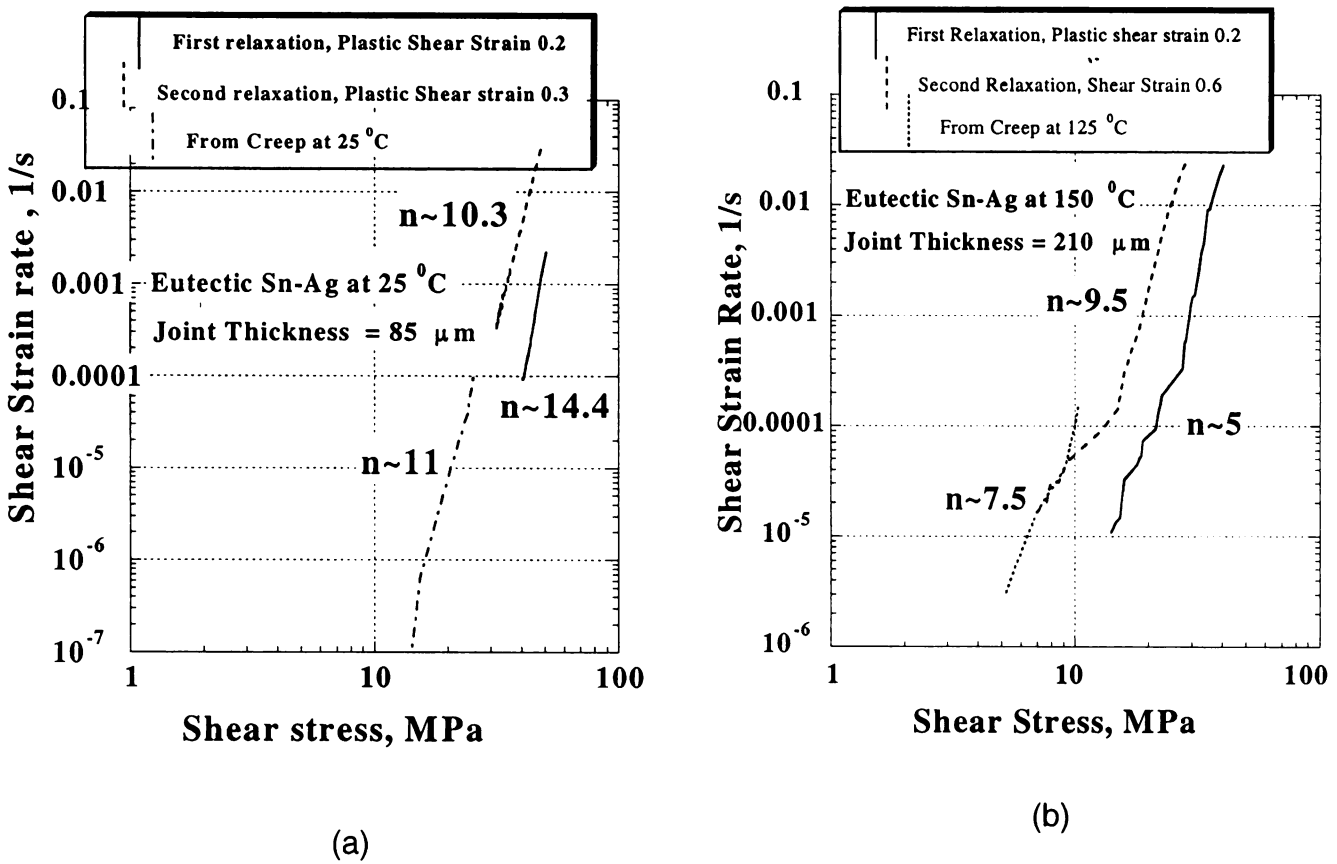

Figure 25. Log strain rare versus log stress plots for eutectic Sn-Ag (a) at 25°C and (b) at 150°C.

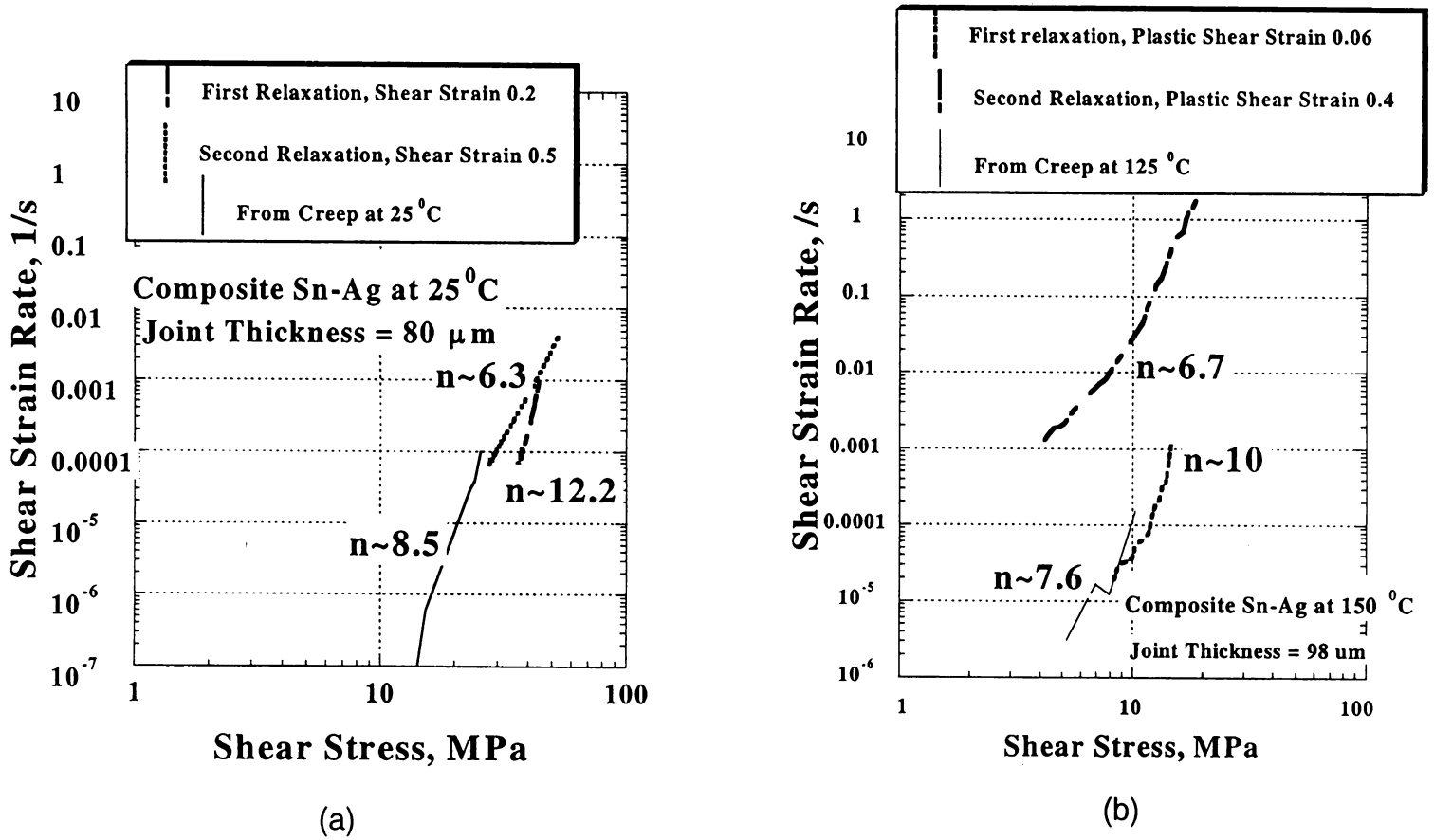

Figure 26. Log strain rate versus log stress plots for a composite solder (a) at 25°C and (b) at 150°C.

The stress exponents obtained during relaxation at high temperature are lower than the stress exponents at low temperature for eutectic and composite solder joints (**Figures 25 and 26**). This is consistent with the results obtained from the conventional creep experiments reported elsewhere in the literature by Choi *et al.* [42]. Stress exponent values obtained in **Figures 25 and 26** are large i.e. above 7. High stress exponents are commonly observed for dispersion-strengthened alloys. According to Murthy *et al.* [43] eutectic Sn-Ag can be regarded as a dispersion-strengthened alloy because of the presence of finely dispersed Ag_3Sn intermetallics in the Sn matrix. The finely dispersed Ag_3Sn intermetallics act like dispersoids that can block dislocation glide and climb. In this case, the creep deformation is controlled by the climb of dislocation loops over the dispersoid particles.

Dislocation density and recovery

The shear strain rates computed from sequential relaxation experiments carried out on the same specimen are different (**Figures 25, 26** and **27**). The strain rate is higher for a larger prior shear strain. According to Orowan [44] the plastic strain rate is related to the mobile dislocation density through the equation,

$$\dot{\varepsilon}_p = K\rho_m bv ,$$

where $\dot{\varepsilon}_p$ is the plastic strain rate, ρ_m is mobile dislocation density, b is Burger's vector, v is average dislocation velocity and K is a constant.

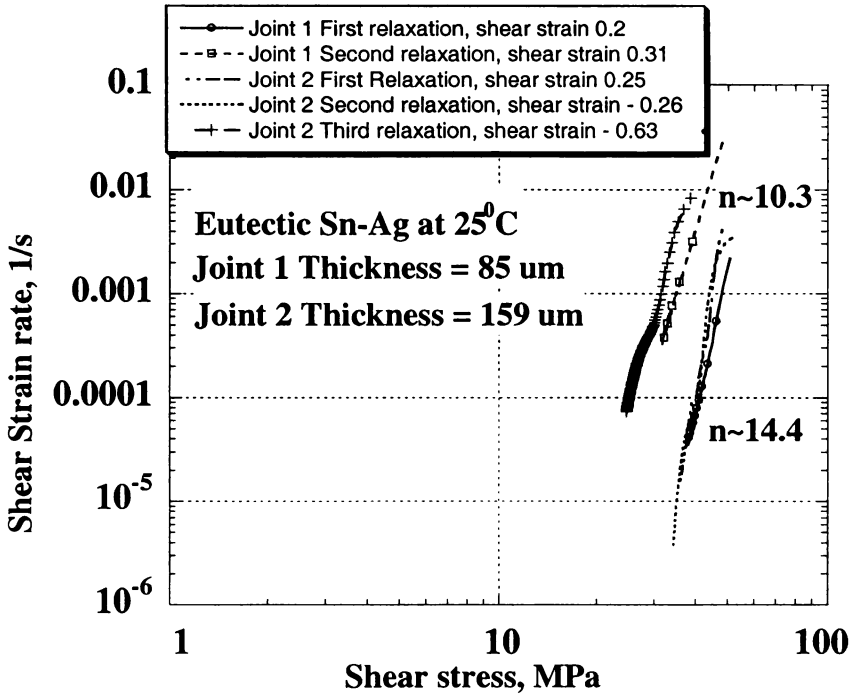

Figure 27. Log$\dot{\gamma}$ vs. logτ plots for eutectic Sn-Ag joints at 25°C.

From **Figures 25** and **26** it is observed that a greater amount of plastic prestrain leads to a greater which shows that the plastic strain rate increases with increasing shear strain in relaxation with different samples. The same trend is seen in **Figure 27**. Thus with greater amount of prestrain a higher mobile dislocation density is achieved. During relaxation, especially at high temperatures (>0.5 T_m) these dislocations rearrange themselves through the process of recovery. Earlier works by Solomon and Nix [45] and Lloyd and McElroy [46] show that mobile dislocation density changes during stress relaxation process. A higher initial mobile dislocation density obtained with a greater prestrain is likely to contribute more opportunity for recovery to occur by rearrangement of dislocations during relaxation resulting in a greater % of stress drop. The higher creep rate obtained with a large prestrain is line with conventional creep data [42].

However, during high temperature relaxation (**Figures 25b and 26b**), the relative creep rates of the composite and the eutectic are very different and they are also different from the conventional creep rate data at high temperature. For the eutectic joints, the creep rate during relaxation at 150^{0}C is lower or similar to the conventional creep at 125^{0}C implying that the dislocation density prior to relaxation in the eutectic alloy was low. The lower creep rate of eutectic alloy might have resulted from dynamic recovery during the prestrain. In contrast, the composite apparently had a much higher dislocation density just prior to

relaxation resulting in a higher creep rate. This implies that the reinforcements inhibited the dynamic recovery during the loading prior to relaxation.

Microstructural Analysis

Microstructure of the solder joints that underwent stress relaxation were examined under the SEM. The microstructures given in **Figure 28** illustrate that there is extensive inhomogeneous deformation in the eutectic solder joint. The gradual formation of shear bands progresses with each relaxation test. **Figure 29** shows deformation in the composite solder joint indicating debonding between the matrix and the Cu_6Sn_5 reinforcements.

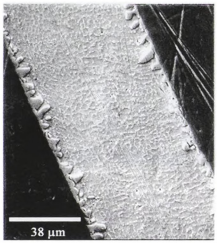

(a)

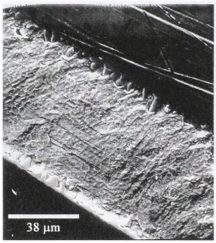

(b)

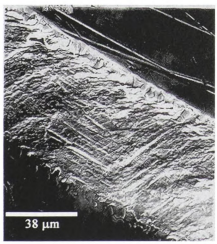

(c)

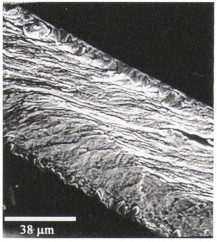

(d)

Figure 28. Microstructure of a Sn-Ag eutectic solder joint subjected to sequential stress relaxation tests at 25°C. (a) As joined (b) after the first relaxation test (shear strain – 0.24) (c) after the second relaxation test (shear strain –0.29) and (d) after the third relaxation test (shear strain –0.28). The magnitude of shear strain imposed prior to each relaxation is shown on the top of each micrograph. Inhomogeneous deformation leading to gradual formation of shear bands with every relaxation can be seen.

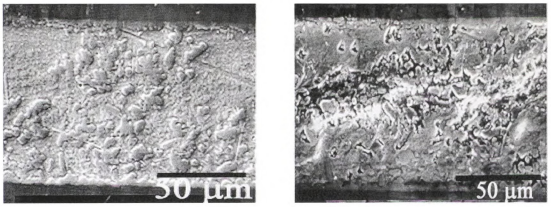

(a) (b)

Figure 29. Microstructure of a composite solder joint subjected to relaxation a 25°C. (a) As joined (b) after first relaxation test (shear strain- 0.37). Relaxed microstructure shows debonding between the Cu_6Sn_5 particles and the matrix. Magnitude of shear strain imposed is shown on the top of the micrograph.

CONCLUSIONS

1. The % stress drop obtained in 1 hour during a relaxation event increases with increasing plastic shear strain imposed prior to relaxation for eutectic Sn-Ag and composite Sn-Ag solder joints tested at 25°C and 150°C.
2. For sequential stress relaxation that includes unloading, the stress drop obtained in 1 hour during a relaxation event is nearly independent of the accumulated plastic shear strain for eutectic Sn-Ag and composite Sn-Ag solder joints. However, for sequential stress relaxation that does not involve unloading, the stress relaxation is dependent upon the cumulative plastic shear strain.
3. The constraints imposed on the solder in shear hinder the complete stress relaxation and significant amount of stress could be retained within the solder joint even after 20 hours at high temperatures as compared to the complete relaxation in experiments with tensile specimens at high temperatures.
4. The strain rate during relaxation increases with increasing imposed prior plastic shear strain.
5. The stress exponent values decrease with increasing temperature for eutectic Sn-3.5Ag and composite Sn-Ag solder joints. The stress exponent values greater than 6 were obtained from relaxation tests suggesting that the deformation mechanism during the stress relaxation at 25°C and at 150°C in eutectic Sn- Ag and composite Sn-Ag solder may be controlled by the dislocation climb recovery processes.

RECOMMENDATIONS

1. In order to investigate the role of recovery processes in solder joint stress relaxation *in-situ* microstructural characterization during relaxation is recommended.
2. Further microstructural studies are necessary to obtain the experimental evidence of change in the dislocation substructure during stress relaxation.
3. Further studies are need to quantify the damage sustained by the joint during stress relaxation and it's effect on the thermomechanical fatigue life of the solder joint.

REFERENCES

1. Abtew M. and Selvaduray G., Materials Science and Engineering, ***R27,*** 2000, p.95.

2. Wassink K. J. R. and Verguld M. M .F., *Manufacturing techniques for Surface Mounted Assemblies*, Electrochemical Publication Limited,1995,GB-Port Erin, British Isles, p.17.

3. Plumbridge W. J., Journal of Materials Science, **31**,1996, p.2501.

4. Boas W. and Honeycombe R. W. K., *Proceedings of the Royal Society A*, **186**, 1945, p.57.

5. Morris J. W. Jr., Goldstein J. L .F. and Mei Z., Journal of Electronic Materials, **22**, 1993, p.25.

6. Glazer J., International Materials Reviews, **40**, 1995, p.65-93.

7. Frear J. R. and Morris J. W., Journal of Electronic Materials, **21**, 1992, p. 647.

8. Darveaux R. and Banerji K., IEEE Transactions on components, Hybrids and Manufacturing,**15**, 1992, p.1014.

9. Weinbel R. C., Tien J. K., Pollak R.A. and Kang S. K., Journal of Materials Science, **22**,1987, p. 3901.

10. Vaynman S., Fine M. E., and Jeannotte D. A., Metallurgical Transactions, **19A**, 1988, p.1051.

11. Attarwala A. I., Tien J. K., Masda G. Y. and Gody G., Journal of Electronic Packaging, **114**,1992, p.109.

12. Tien J. K., Hendrix B. C. and Attarwala A. I., ASME Journal of Electronic Packaging, **113**,1991, p.115.

13. Weinbel R.C., Schwarzkopf E.A. and Tien J.K., Scripta Met., **21**,1987, p. 1165.

14. Dasgupta A., *Handbook of Electronic Packaging,* Edited by Michael Pecht, Morris Dekker, New York, 1991, p.495.

15. Raeder C.H., Messler R. W. Jr. and Coffin L. F. Jr., Journal of Electronic Materials, ***28***, No.9,1999, p.1045.

16. Subramanian K. N., Bieler T. R. and Lucas J. P., Journal of Electronic Materials, **28**,1999, p.1176.

17. Frear D. R., Proceedings of the 40th ECTC Conference, Las Vegas, NV, IEEE,1990, p.510.

18. Lawson L.R., *Ph. D. Thesis,* North Western University, 1989.

19. Keller H.N., IEEE Components, Hybrid Manufacturing Technology, IEEE CHMT-4, 1981, p.492.

20. Karjalainan L. P., Rautioaho R. H., Jarvenpaa S. A., Rikola R. and Vahakngas J., Brazing and Soldering, **15**, 1988, p.37.

21. Frear D. R., *Solder Mechanics-A State of the Art Assessment*, Edited by Frear D. R., Jones W. B. and Kinsman K. R., TMS, Warrendale, PA, p.191.

22. Solomon H. D., *Electronic Packaging: Materials and Processes, Edited by Sortell J. A.,* ASM, Metals Park, Ohio, 1985, p.29.

23. Li J.C.M., Journal of Electronic Materials, **26**,1997, p.827.

24. Geckinli A. E. and Barrett C. R., Scripta Metallurgica, **8**, 1974, p.115.

25. Dasgupta A., *Handbook of Electronic Packaging,* Edited by Michael Pecht, Morris Dekker, New York, 1991, p.501.

26. Vaynman S., Fine M. E. and Jeannotte D. A, *Proceedings of the 3rd Annual Electronic Packaging and Corrosion in Microelectronics Conference,* edited by Nicholson M. E.,ASM International,1987, p.169.

27. Hare E.W. and Stang R. G., Journal of Electronic Materials, **24**, 10,1995, p.1474.

28. Frost H.J., *Microelectronic Technology and Processes, edited by W.T. Shieh,* ASM International, Materials Park, Ohio, 1989, p.121.

29. Solomon H. D. and Talksdorf E. D., ASME Journal of Electronic Packaging, **118**, 1995, p.66.

30. Solomon H.D., *Proceedings of 3rd ASM International Conference on Electronic Materials and Processes Congress*, San Francisco, *CA,* 1990, p.187.

31. Choi S., Bieler T. R., Subramanian K.N. and Lucas J. P., Journal of Electronic Materials, **29**,10,2000,p.1249.

32. Baker E., Materials Science and Engineering, **38,** 1979, p.241.

33. Murty G.S., Journal of Materials Science Letters, **8**,1973, p.611.

34. Kashyap B. P. and Murty G. S., Metallurgical Transactions, **12A**, 1981, p.1923.

35. Rohde R. W. and Swearengen J. C., Journal of Engineering Materials and Technology, **102**, 1980, p.207.

36. Arrowood R. and Mukherjee A. K., Materials Science and Engineering, **92**,1987, p.33.

37. Mavoori H., Chin J., Vaynman S., Moran B., Keer L. and Fine M., Journal of Electronic Materials, **26**, 1997, p.784.

38. Cagnon M., Suery M., Eberhardt A. and Baudelet B., Acta Metallurgica, **25**,1977, p.71.

39. Nix W. D. and Gibeling J. C., *ASM Materials Science Seminar,* Philadelphia, USA, edited by Rishi Raj, ASM, Metals Park, Ohio, 1985, p.1.

40. Lucas J. P., Guo F., Mcdougall J., Bieler T. R., Subramanian K.N. and Park J.K., Journal of Electronic Materials, **28,** 1999, p.1209.

41. Darveaux R. and Turlik I., *Proceedings of 1990 Intersociety Conference on Thermal Phenomena in Electronic Systems*, (I-Therm II), Las Vegas, USA, 1990, IEEE, p. 40.

42. Choi S., Lee J.G., Guo F., Bieler T.R., Subramanian K.N. and Lucas J.P., *to be published* in Journal of Metals.

43. K. Linga Murthy, Yang H., Deane P. and Magill P., Advances in Electronic Packaging, **1** (1997), p.1221.13.

44. Orowan E., *Proceedings of Physical Society*, **52**, 8, 1940, p.1.

45. Solomon A.A. and Nix W.D., *Acta Metallurgica*, **18**, 1970, p.863.

46. Lloyd G.J. and McErloy R.J., *Acta Metallurgica*, **22**, 1974, p.339.